Mainshock: M 7

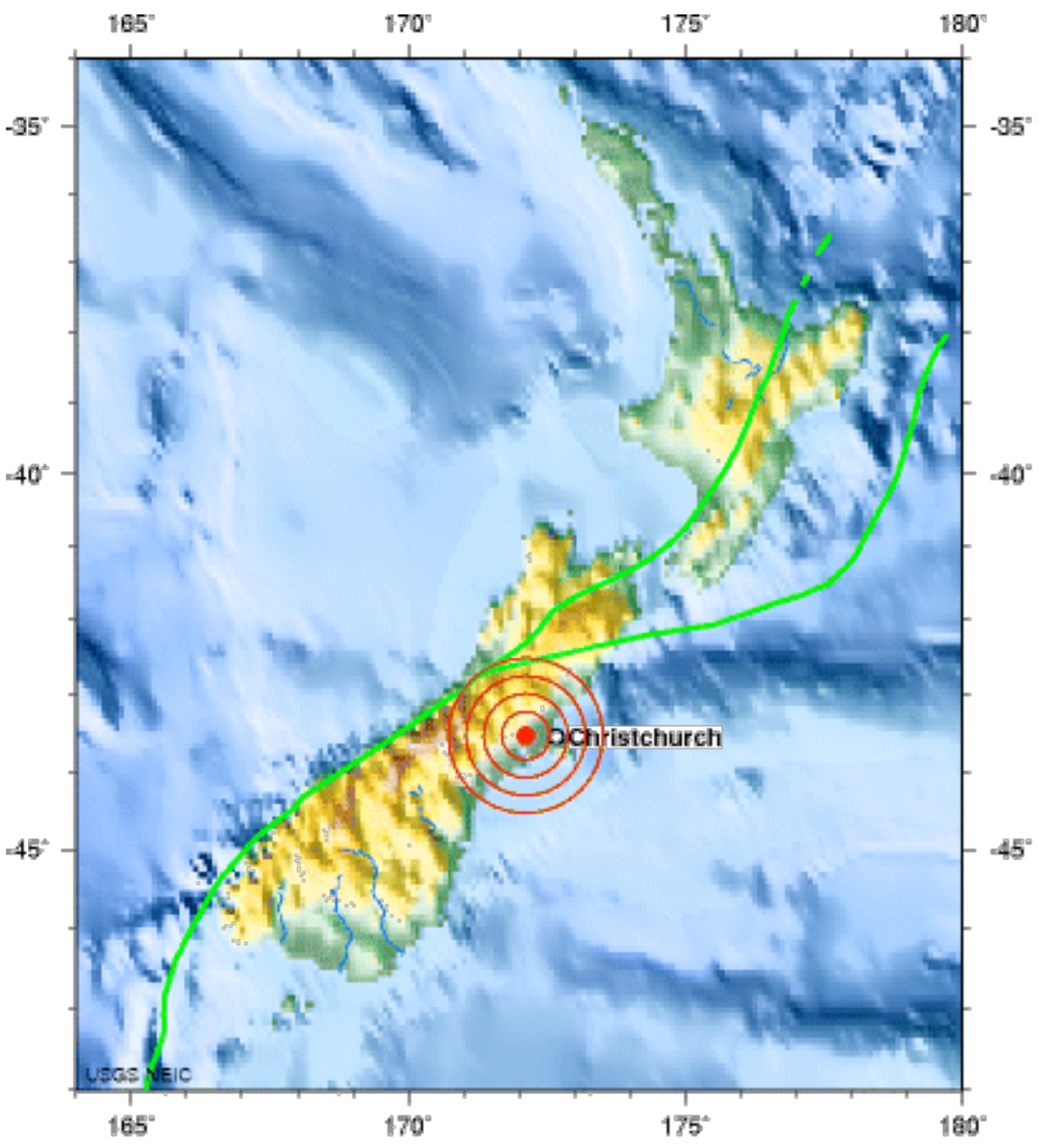

Darfield NZ Sept 3, 2010

Aftershock: M 6.3

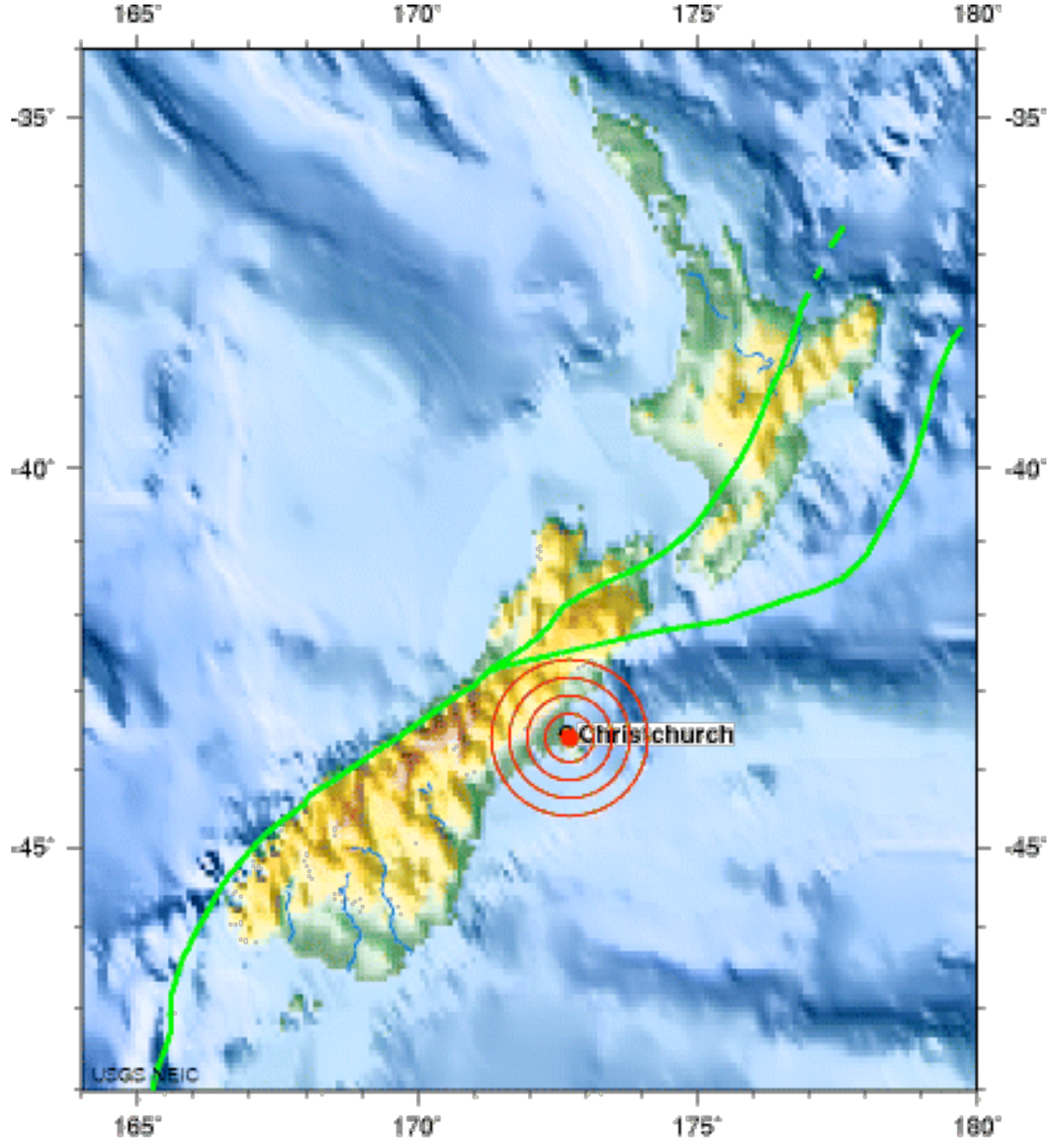

Christchurch NZ Feb 22, 2011

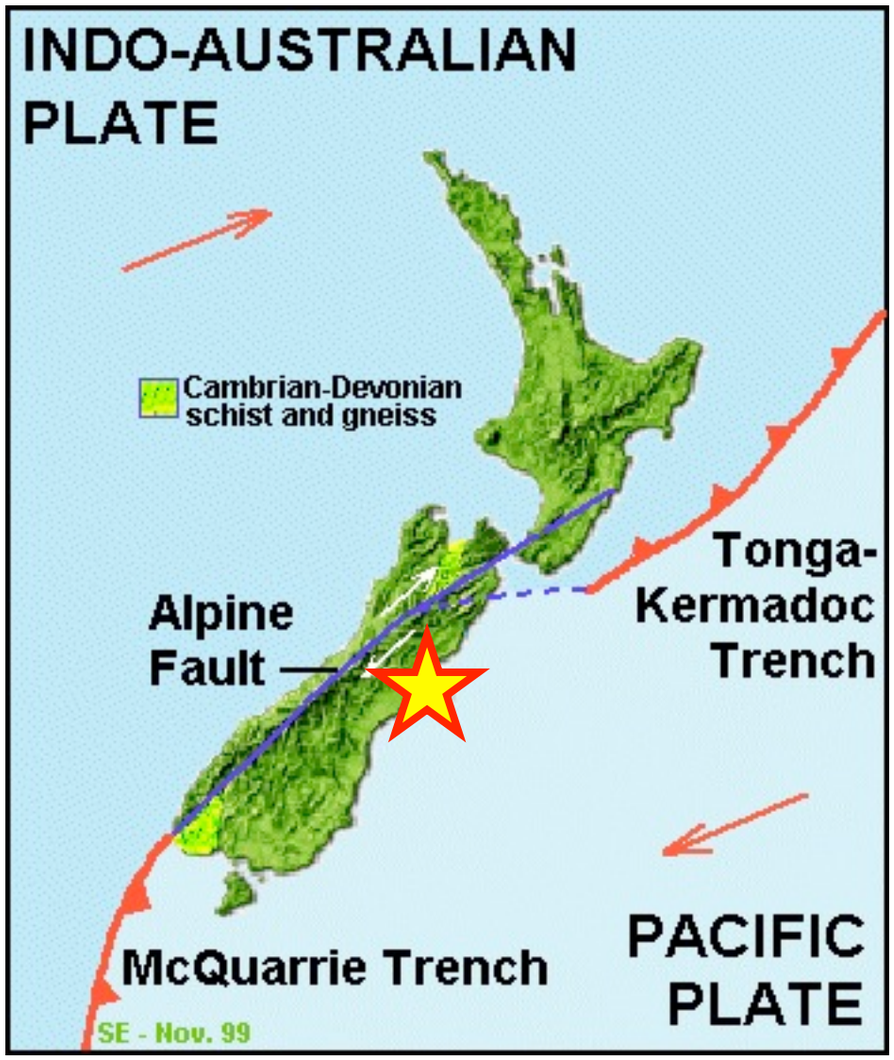


```
CENTROID-MOMENT-TENSOR  SOLUTION
GCMT EVENT:     C201102212351A
DATA: II IU CU IC GE G
L.P.BODY WAVES:103S, 224C, T= 40
MANTLE WAVES:   89S, 133C, T=125
SURFACE WAVES: 101S, 209C, T= 50
TIMESTAMP:      Q-20110221212041
CENTROID LOCATION:
ORIGIN TIME:      23:51:47.8 0.1
LAT:43.61S 0.01;LON:172.54E 0.01
DEP: 12.0  FIX;TRIANG HDUR:  2.8
MOMENT TENSOR: SCALE 10**25 D-CM
RR= 1.090 0.015; TT= 0.608 0.016
PP=-1.690 0.014; RT= 0.534 0.039
RP= 0.012 0.037; TP=-1.230 0.014
PRINCIPAL AXES:
1.(T) VAL=  1.608;PLG=44;AZM= 20
2.(N)       0.639;    46;    208
3.(P)      -2.240;     4;    114
BEST DBLE.COUPLE:M0= 1.92*10**25
NP1: STRIKE=167;DIP=57;SLIP=  32
NP2: STRIKE= 59;DIP=64;SLIP= 143
```

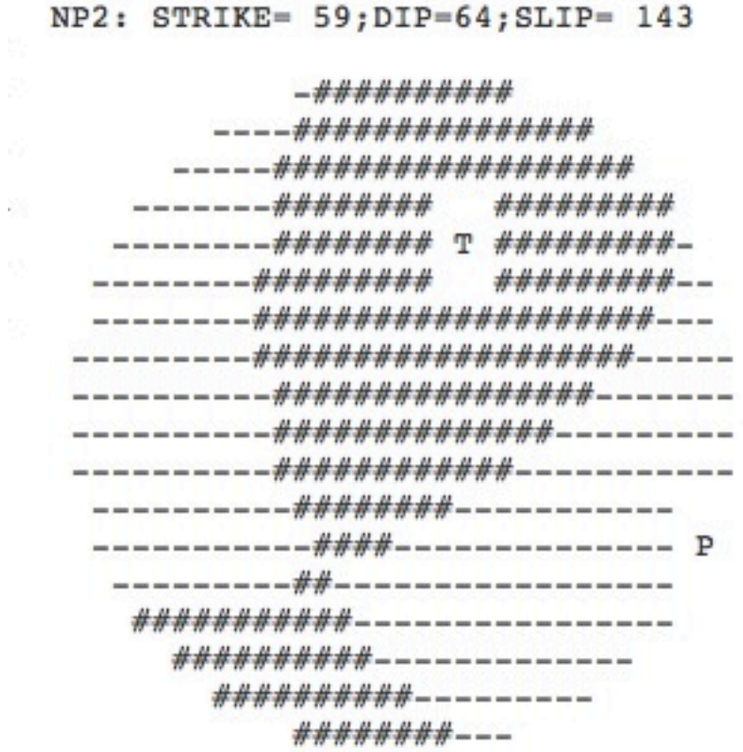

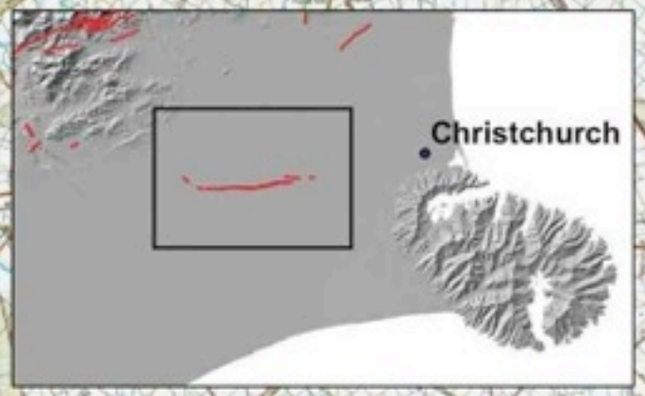

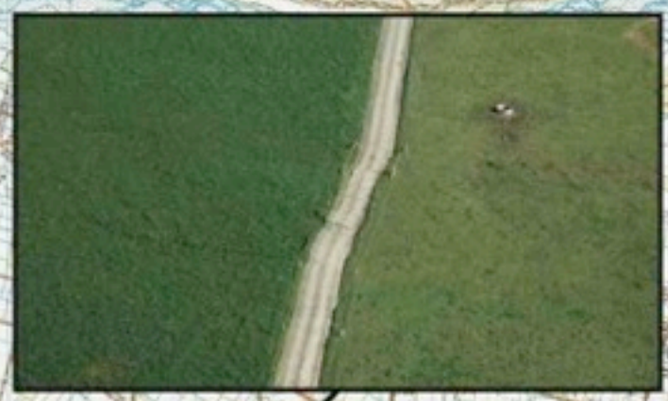

UC UNIVERSITY OF CANTERBURY

GNS SCIENCE

Rolleston

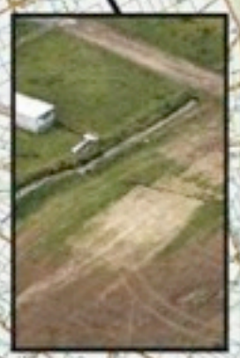

0 5 km

0 5 km

M 7 Darfield Quake from last September

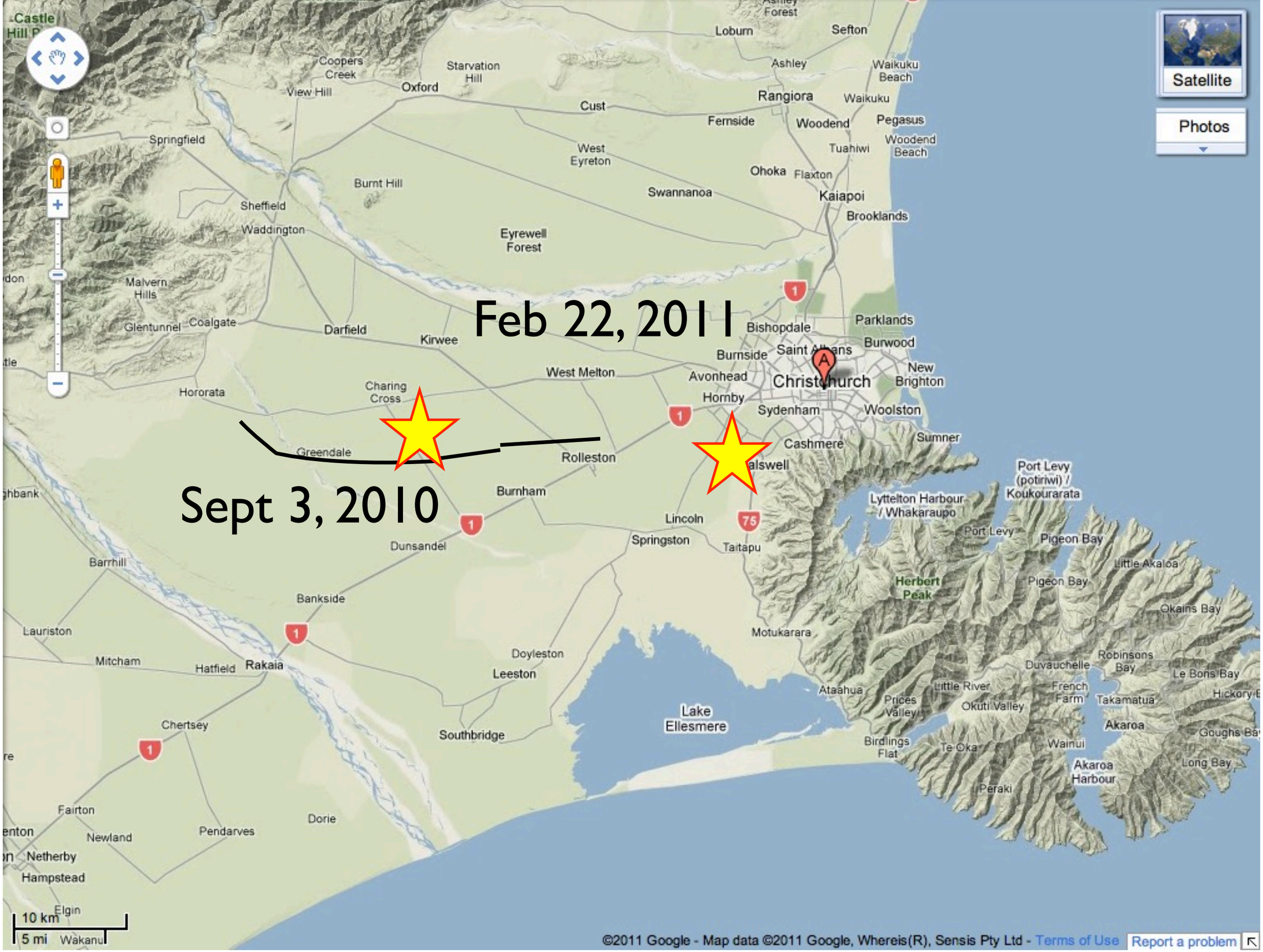
Feb 22, 2011
Sept 3, 2010
Satellite
Photos
Christchurch
Lake Ellesmere
Springfield
Sheffield
Waddington
Malvern Hills
Glentunnel
Coalgate
Darfield
Kirwee
Hororata
Charing Cross
Greendale
Rolleston
West Melton
Burnham
Dunsandel
Barrhill
Bankside
Lauriston
Mitcham
Hatfield
Rakaia
Chertsey
Southbridge
Doyleston
Leeston
Lincoln
Springston
Taitapu
Motukarara
Fairton
Newland
Pendarves
Dorie
Netherby
Hampstead
Elgin
Wakanui
Eyrewell Forest
Burnt Hill
West Eyreton
Swannanoa
Oxford
Coopers Creek
View Hill
Starvation Hill
Cust
Loburn
Sefton
Ashley
Rangiora
Fernside
Waikuku Beach
Waikuku
Woodend
Pegasus
Woodend Beach
Tuahiwi
Ohoka
Flaxton
Kaiapoi
Brooklands
Parklands
Bishopdale
Burwood
Burnside
Saint Albans
Avonhead
New Brighton
Hornby
Sydenham
Woolston
Cashmere
Sumner
Port Levy (potiriwi) / Koukourarata
Lyttelton Harbour / Whakaraupo
Port Levy
Pigeon Bay
Little Akaloa
Herbert Peak
Okains Bay
Robinsons Bay
Le Bons Bay
Duvauchelle
Little River
French Farm
Takamatua
Hickory B
Ataahua
Prices Valley
Okuti Valley
Akaroa
Goughs Bay
Birdlings Flat
Te Oka
Wainui
Akaroa Harbour
Long Bay
Peraki
10 km
5 mi
©2011 Google - Map data ©2011 Google, Whereis(R), Sensis Pty Ltd - Terms of Use
Report a problem

Darfield NZ Sept 3, 2010 Mainshock: M 7

Aftershock: M 6.3 Christchurch NZ Feb 22, 2011

Estimated Population Exposed to Earthquake Shaking

Estimated Modified Mercalli Intensity		I	II-III	IV	V	VI	VII	VIII	IX	X
Est. Population Exposure		---*	---*	161k*	94k	54k	68k	245k	65k	0
Perceived Shaking		Not Felt	Weak	Light	Moderate	Strong	Very Strong	Severe	Violent	Extreme
Potential Structure Damage	Resistant	none	none	none	V. Light	Light	Moderate	Moderate/Heavy	Heavy	V. Heavy
	Vulnerable	none	none	none	Light	Moderate	Moderate/Heavy	Heavy	V. Heavy	V. Heavy

*Estimated exposure only includes population within calculated shake map area

Population Exposure

Population per ~1 sq. km. from LandScan

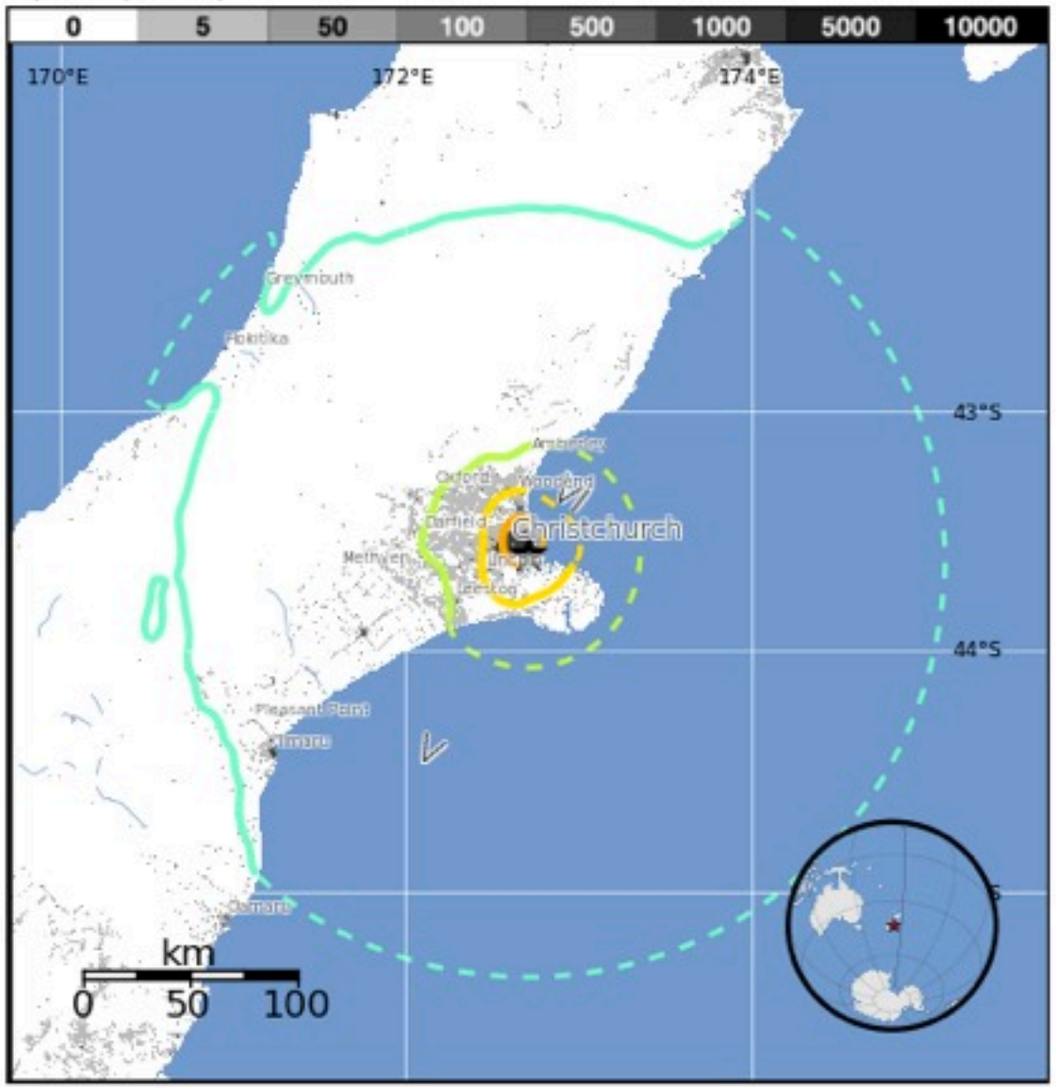

Structure Information Summary

Overall, the population in this region resides in structures that are highly resistant to earthquake shaking, though some vulnerable structures exist. The predominant vulnerable building types are reinforced masonry and concrete/cinder block masonry construction.

Historical Earthquakes (with MMI)

Date (UTC)	Dist (km)	Mag	Max MMI (#)	Shaking Deaths
1984-06-24	164	6.1	VIII (18)	0
1990-02-10	143	6	VIII (61)	0
1994-06-19	100	5.9	VIII (12)	0

Selected Cities Exposed

from GeoNames Database of Cities with 1,000 or more residents.

MMI	City	Population
VIII	Christchurch	364k
VI	Woodend	3k
VI	Lincoln	2k
V	Rolleston	3k
V	Oxford	2k
V	Darfield	2k
IV	Timaru	28k
IV	Blenheim	27k

http://www.youtube.com/watch?v=Wrmj5UVMyII&feature=youtu.be

From GNS New Zealand (accelerometer data)
M 6.3

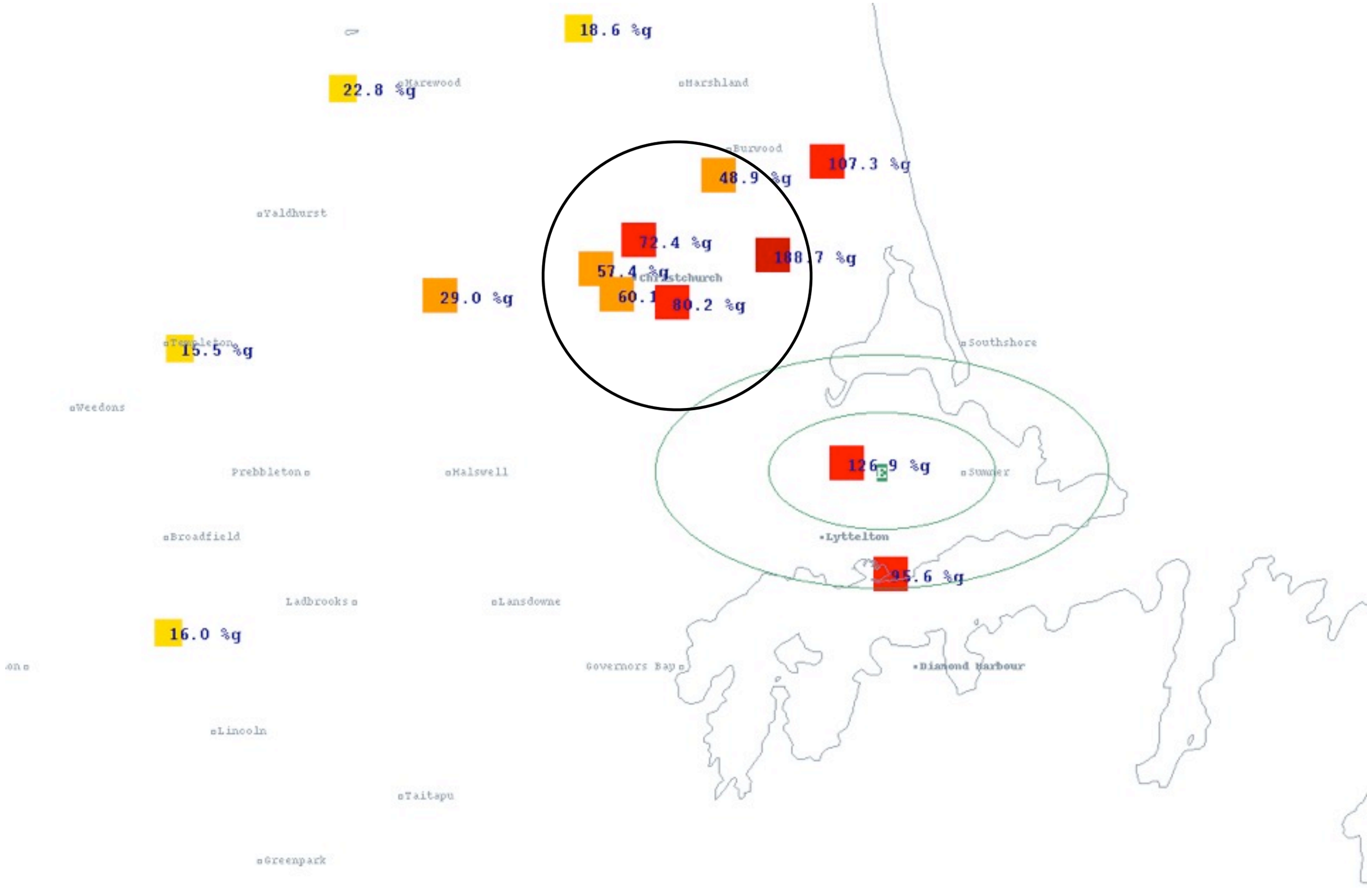

From GNS New Zealand (accelerometer data)

M 7

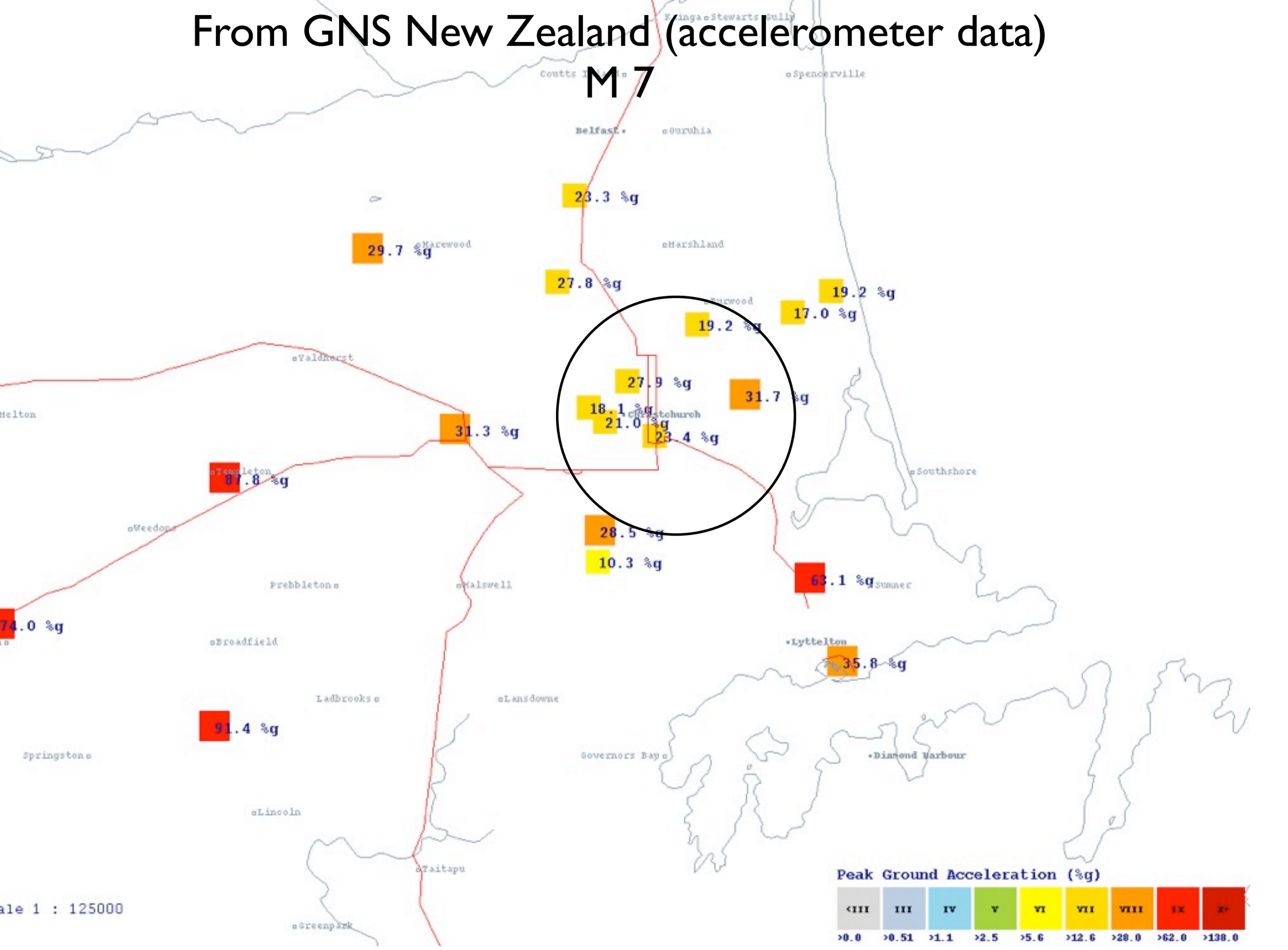

New Zealand Seismograph network

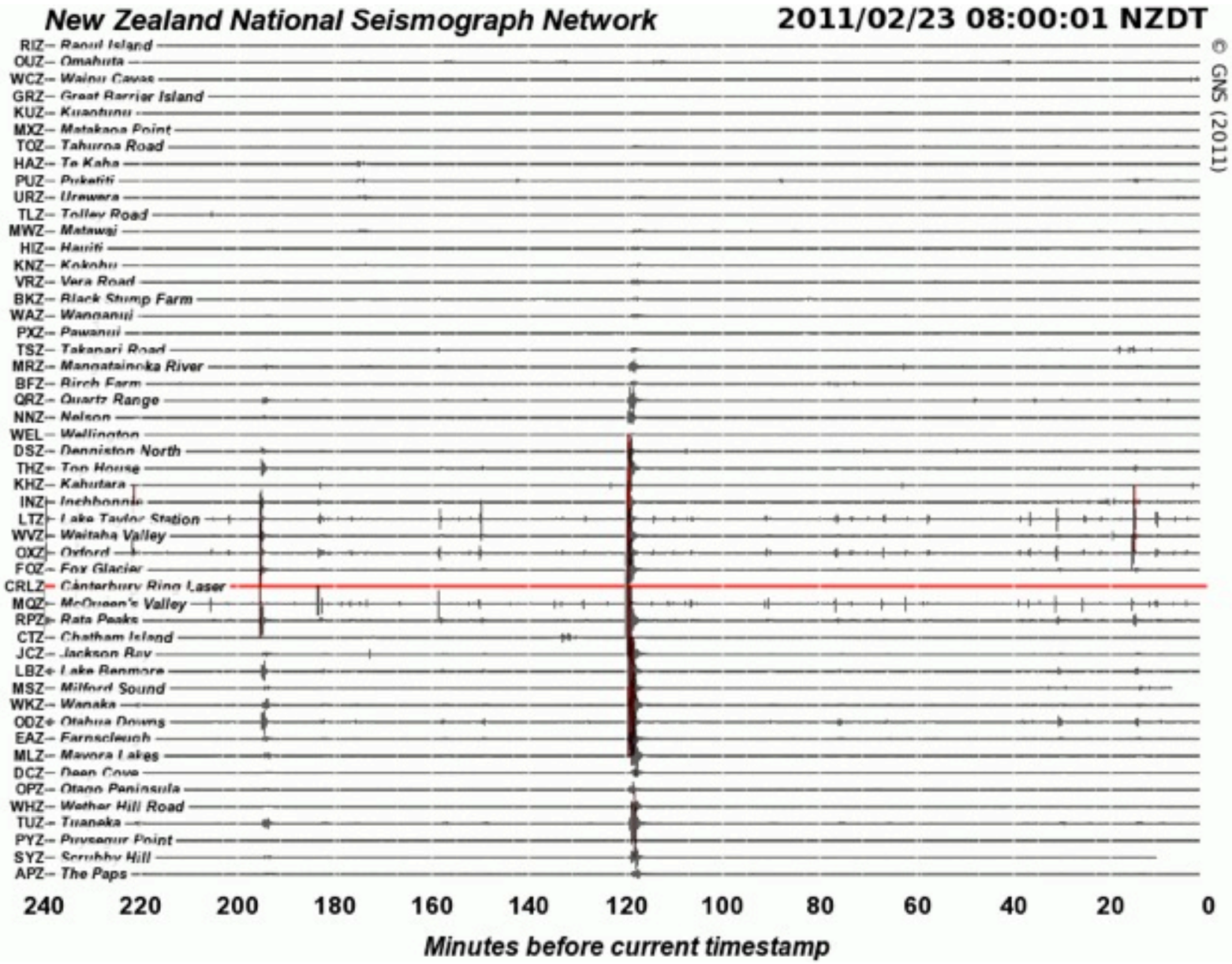

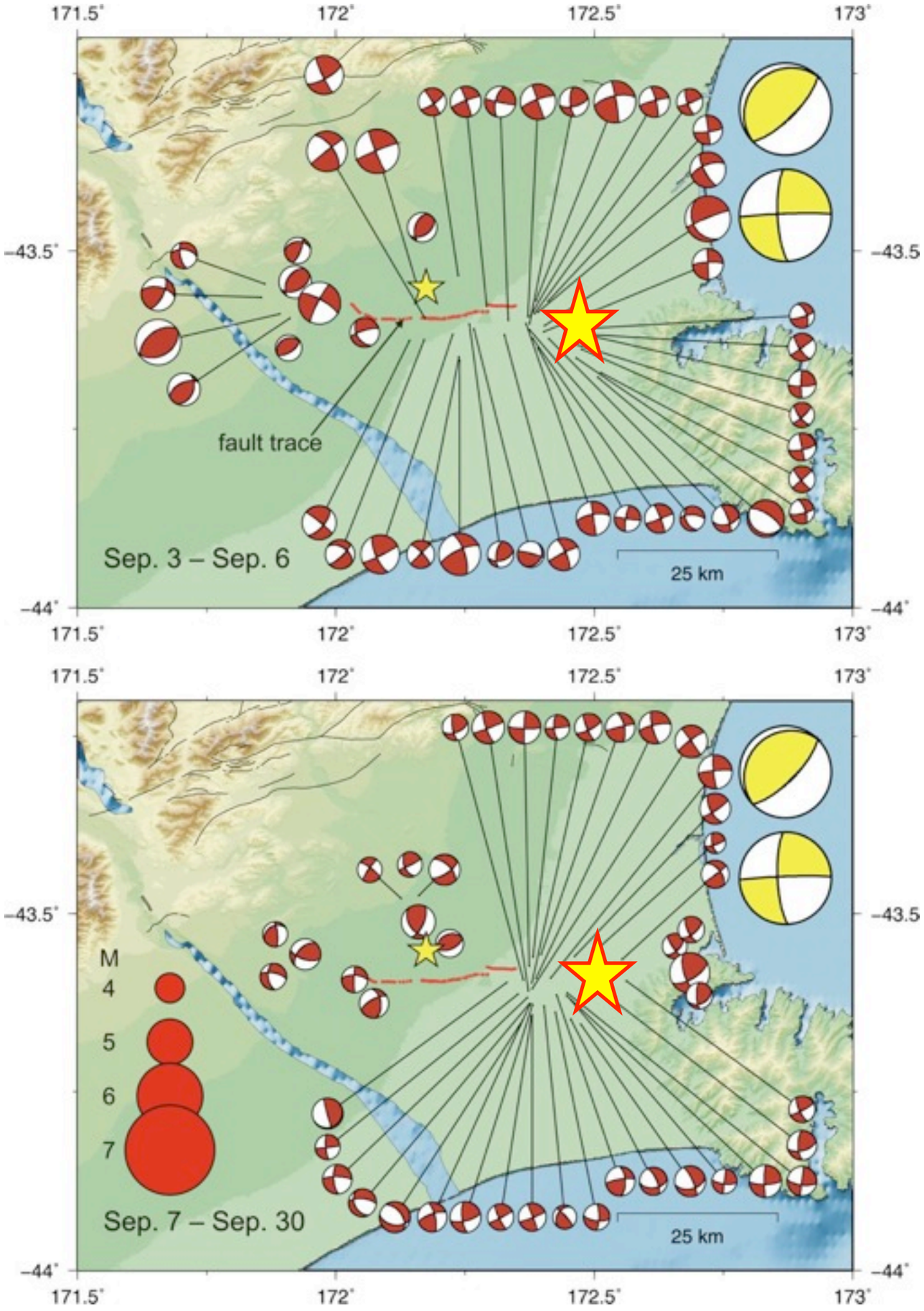
171.5°
172°
172.5°
173°
−43.5°
−44°
fault trace
Sep. 3 – Sep. 6
25 km
M
4
5
6
7
Sep. 7 – Sep. 30

From GNS New Zealand - later part of Darfield aftershock sequence

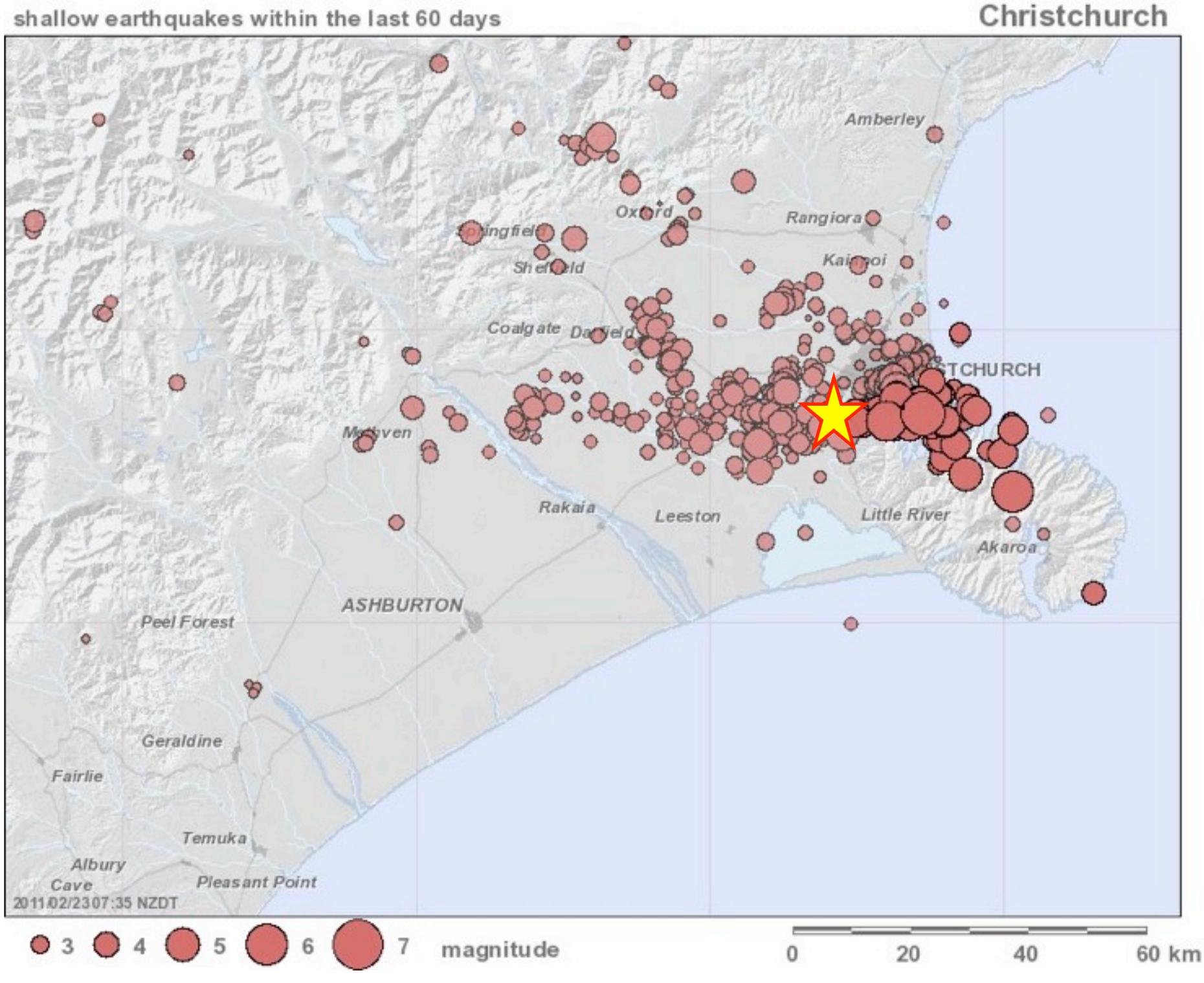

Strong motion I

Strong motion parameters - peak values, Fourier spectra, corner frequency
estimating slipped patch size and stress drop

Response spectra - what are they and what are they for

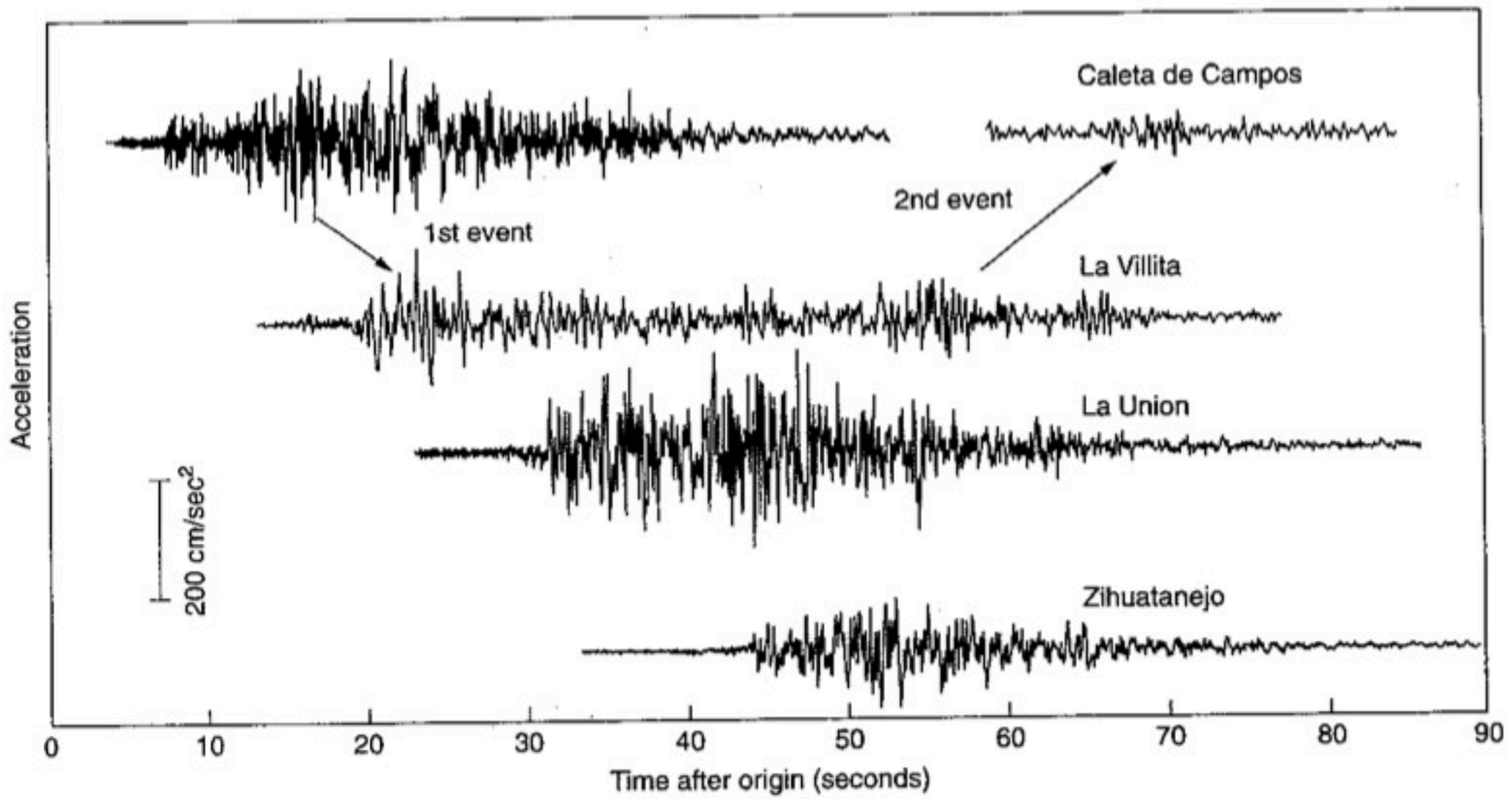

FIGURE 1 North–south component of acceleration at four strong-motion stations that recorded the September 19, 1985, Michoacan, Mexico, earthquake ($M_w = 8.0$). The Caleta de Campos station is almost directly above the hypocenter, the Zihuatanejo station is near the end of the rupture, 146 km east-southeast of Caleta de Campos, and the other stations are approximately along a line between Caleta de Campos and Zihuatanejo. The vertical separation of the traces is proportional to the separation of the stations on a projection along the strike of the causative fault. All records are aligned in absolute time after the origin of the earthquake (from Anderson *et al.*, 1986).

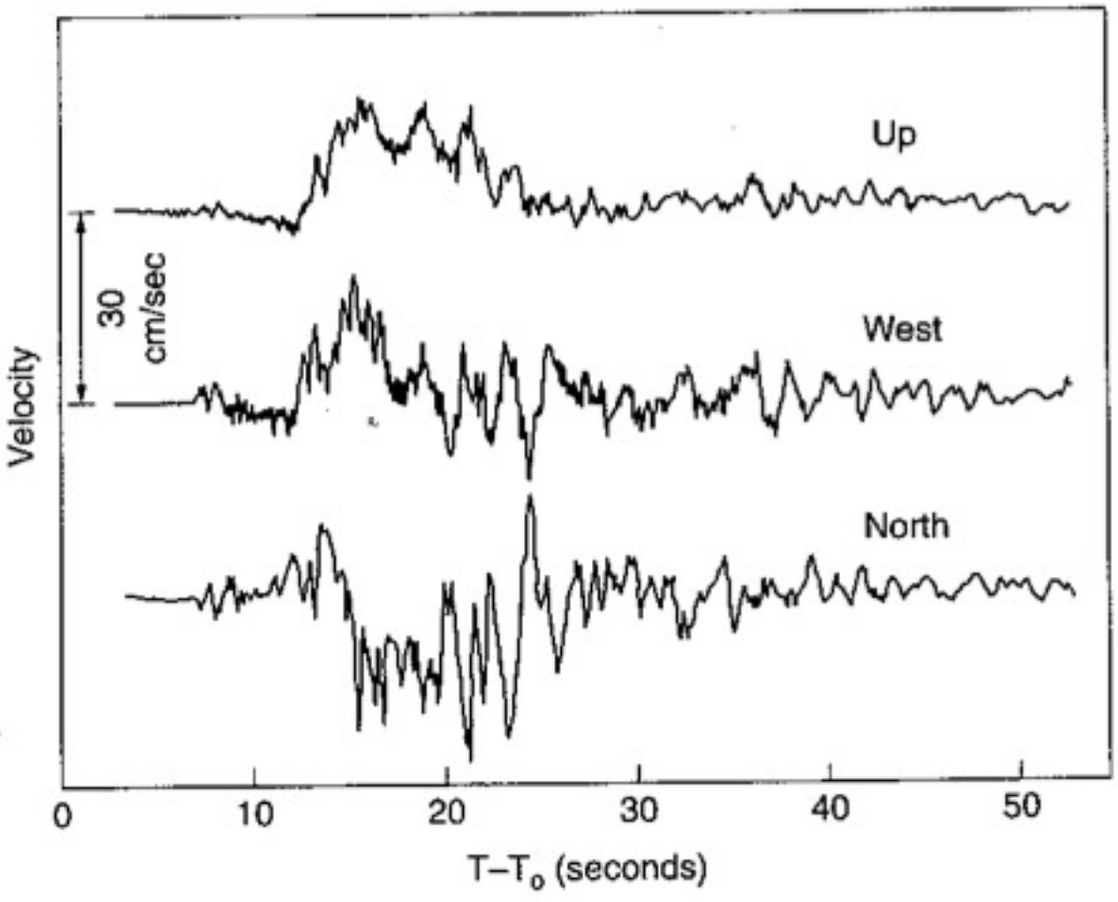

FIGURE 2 Three components of velocity at Caleta de Campos during the September 19, 1985, Michoacan earthquake (from Anderson *et al.*, 1986).

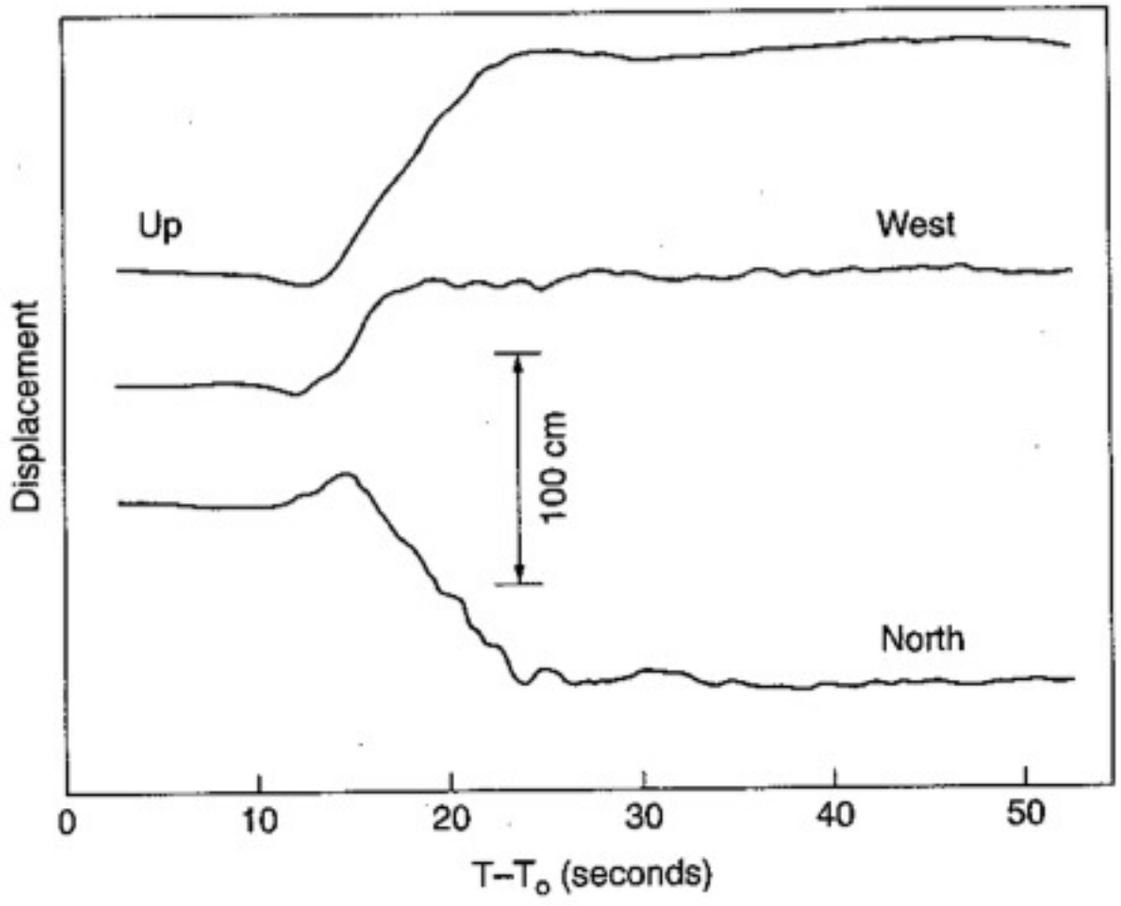

FIGURE 3 Three components of displacement at Caleta de Campos during the September 19, 1985, Michoacan earthquake (from Anderson *et al.*, 1986).

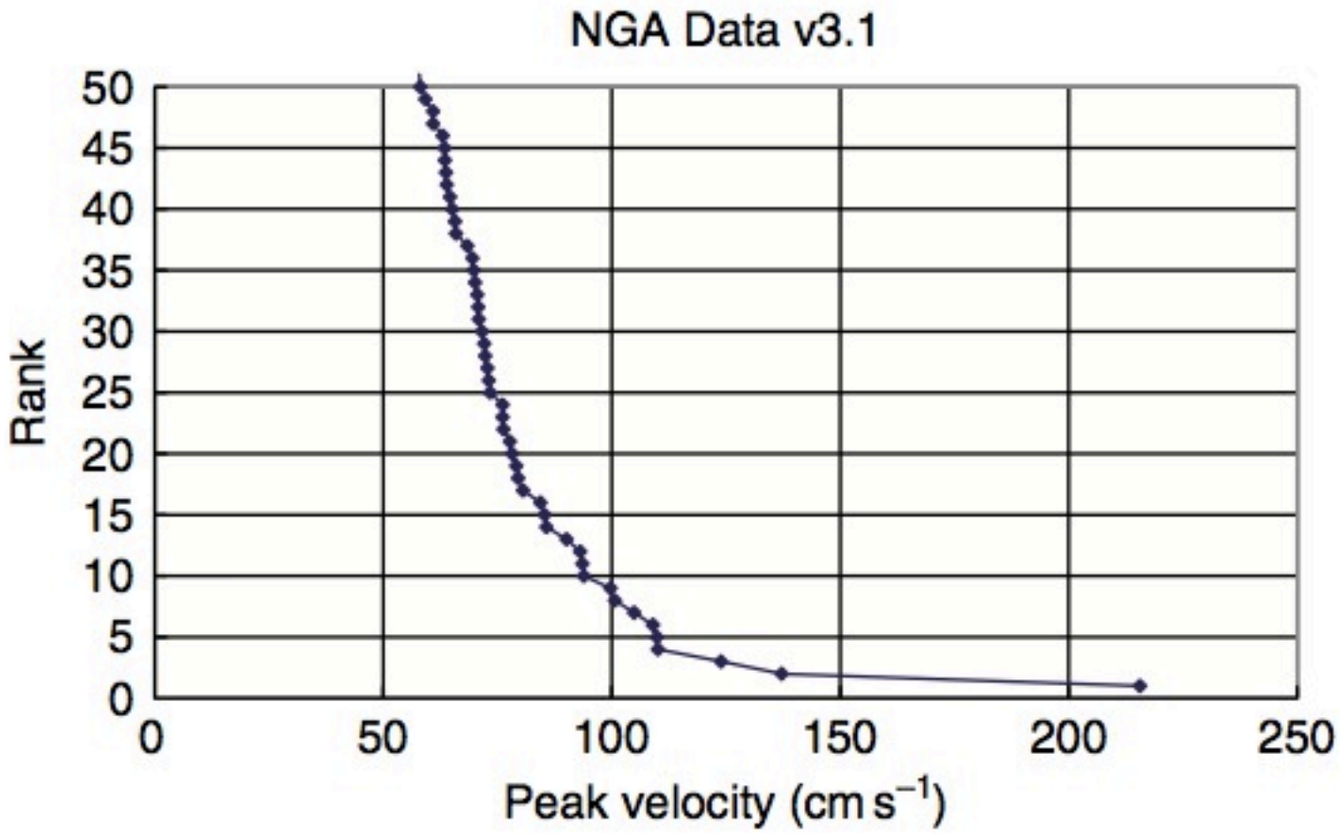

Figure 2 Extreme velocities recorded in free-field conditions. This set of observations with extreme velocity records has been drawn from the PEER NGA database. The peak velocities in this database are the geometric mean of the two horizontal components. On average, these are about 75% of the peak vector velocity. From Anderson JG, Purvance M, Brune JN, and Anooshehpoor A (2005a) Developing Constraints on Extreme Ground Motions Based on Seismic and Geological Observations (extended abstract), 2nd International Workshop, Strong Ground Motion Prediction and Earthquake Tectonics in Urban Areas, 25–27 October, 2005, Earthquake Research Institute, University of Tokyo, Japan, 63–66.

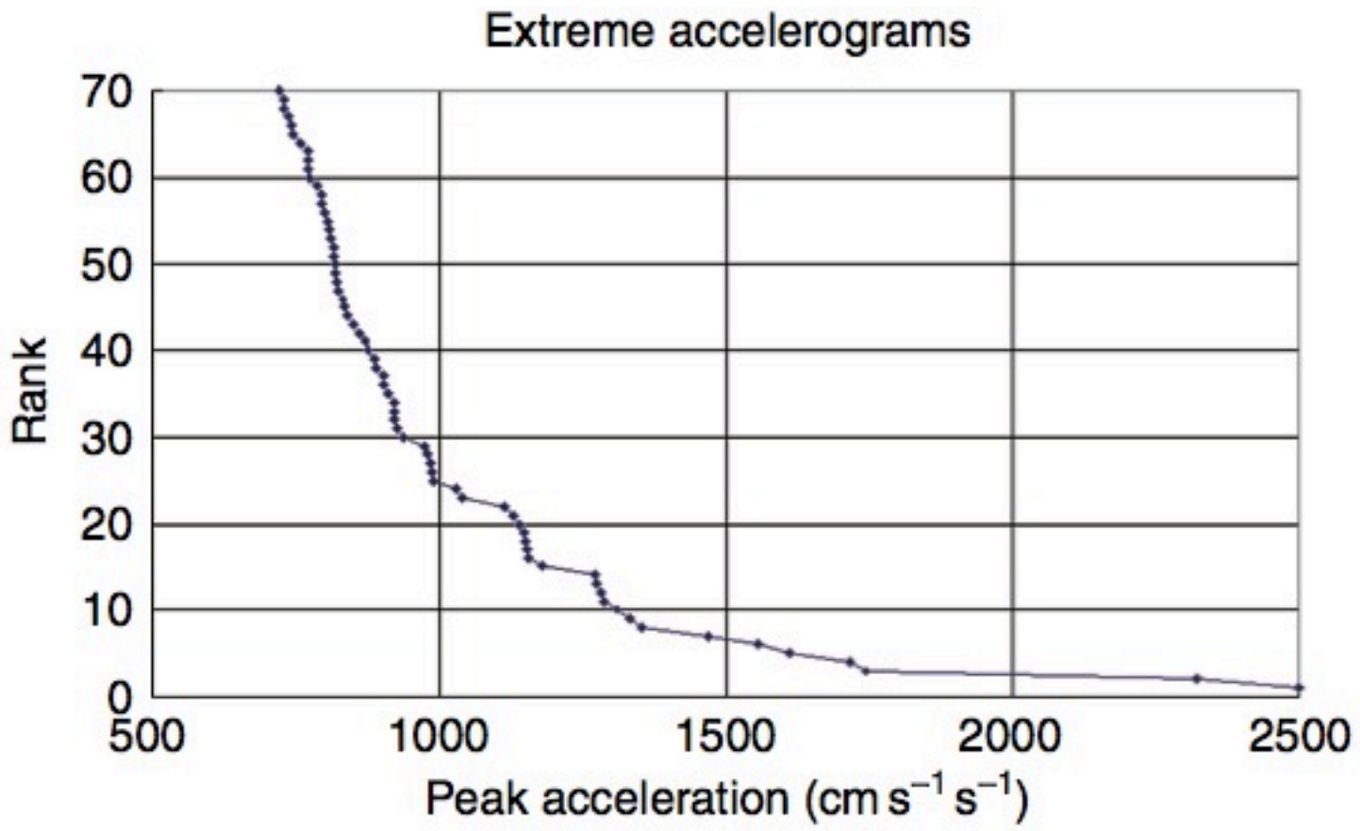

Figure 1 Extreme accelerations recorded in the 'free-field' or in small structures. The table with extreme records has been primarily drawn from the COSMOS Virtual Data Center. Note that these points are all peaks on individual components of strong-motion records. The peak vector acceleration is not necessarily recorded, and statistically its median is 25% greater than the largest horizontal component of a randomly oriented accelerograph. Expanded from Anderson JG, Purvance M, Brune JN, and Anooshehpoor A (2005a) Developing Constraints on Extreme Ground Motions Based on Seismic and Geological Observations (extended abstract), 2nd International Workshop, Strong Ground Motion Prediction and Earthquake Tectonics in Urban Areas, 25–27 October, 2005, Earthquake Research Institute, University of Tokyo, Japan, 63–66.

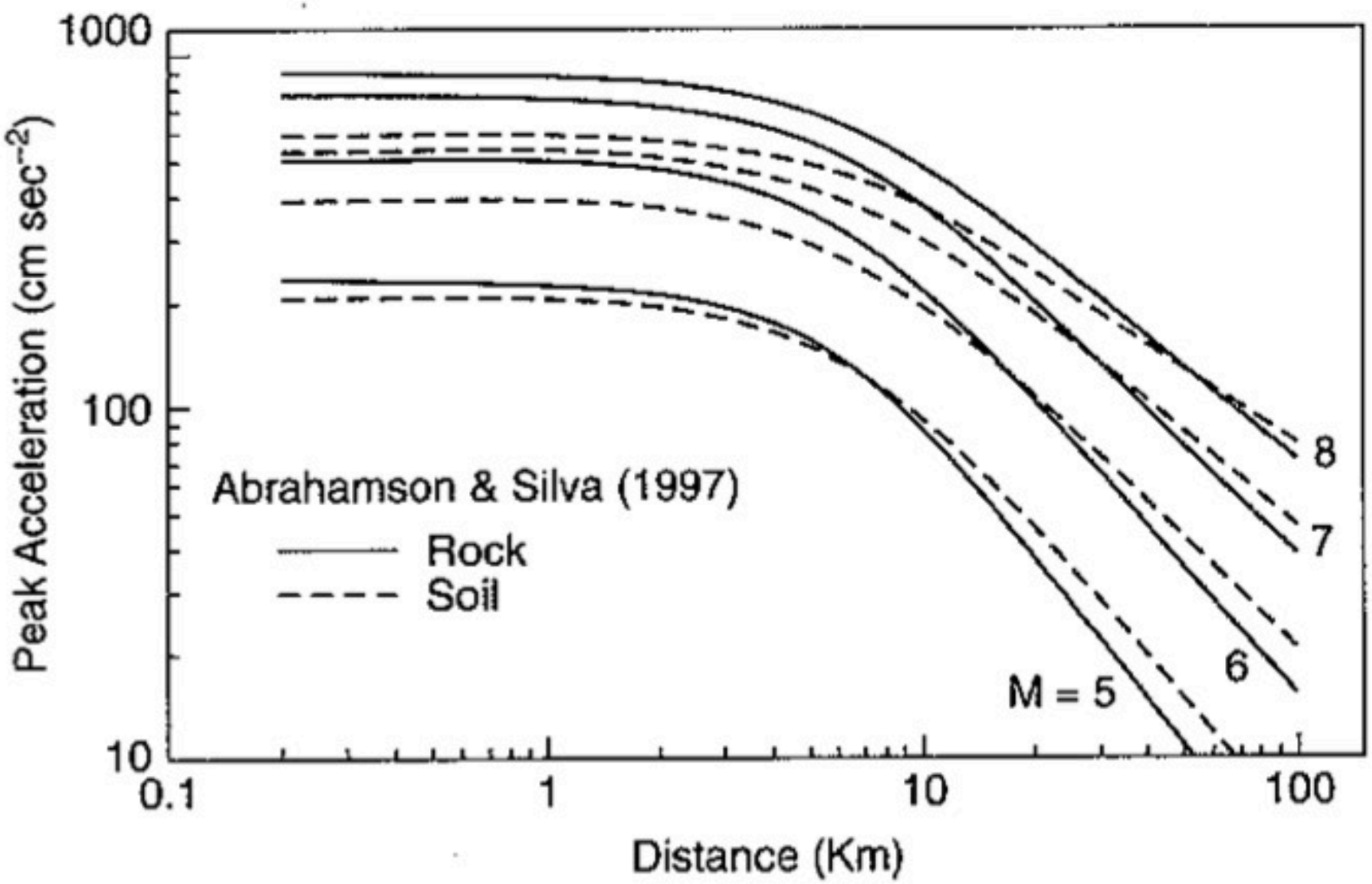

FIGURE 7 Peak acceleration as a function of magnitude and distance from the fault, as given by the ground-motion prediction equation of Abrahamson and Silva (1997).

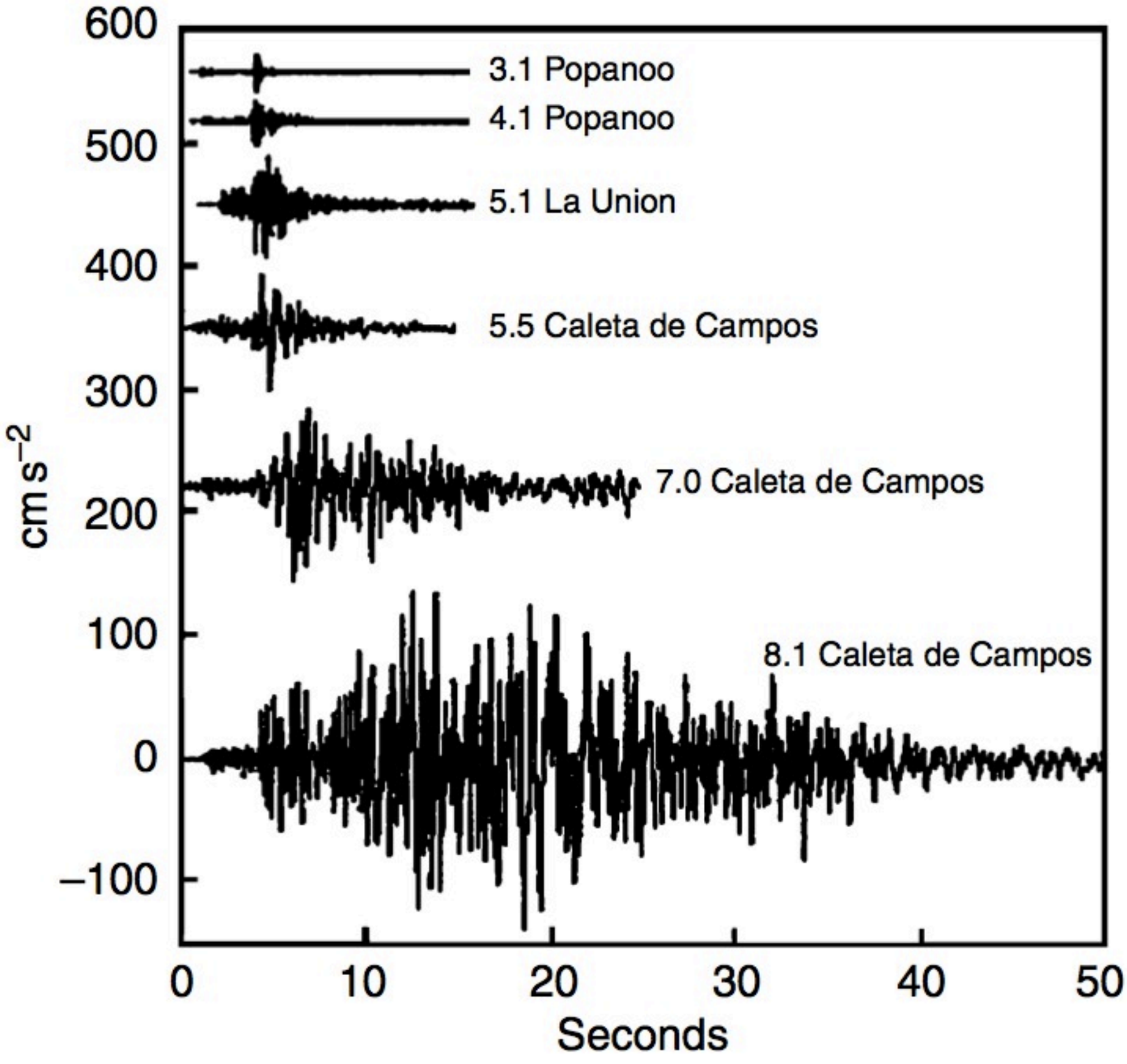
600
500
400
300
200
100
0
−100
cm s−2
3.1 Popanoo
4.1 Popanoo
5.1 La Union
5.5 Caleta de Campos
7.0 Caleta de Campos
8.1 Caleta de Campos
0
10
20
30
40
50
Seconds

Spectra of accelerometer records

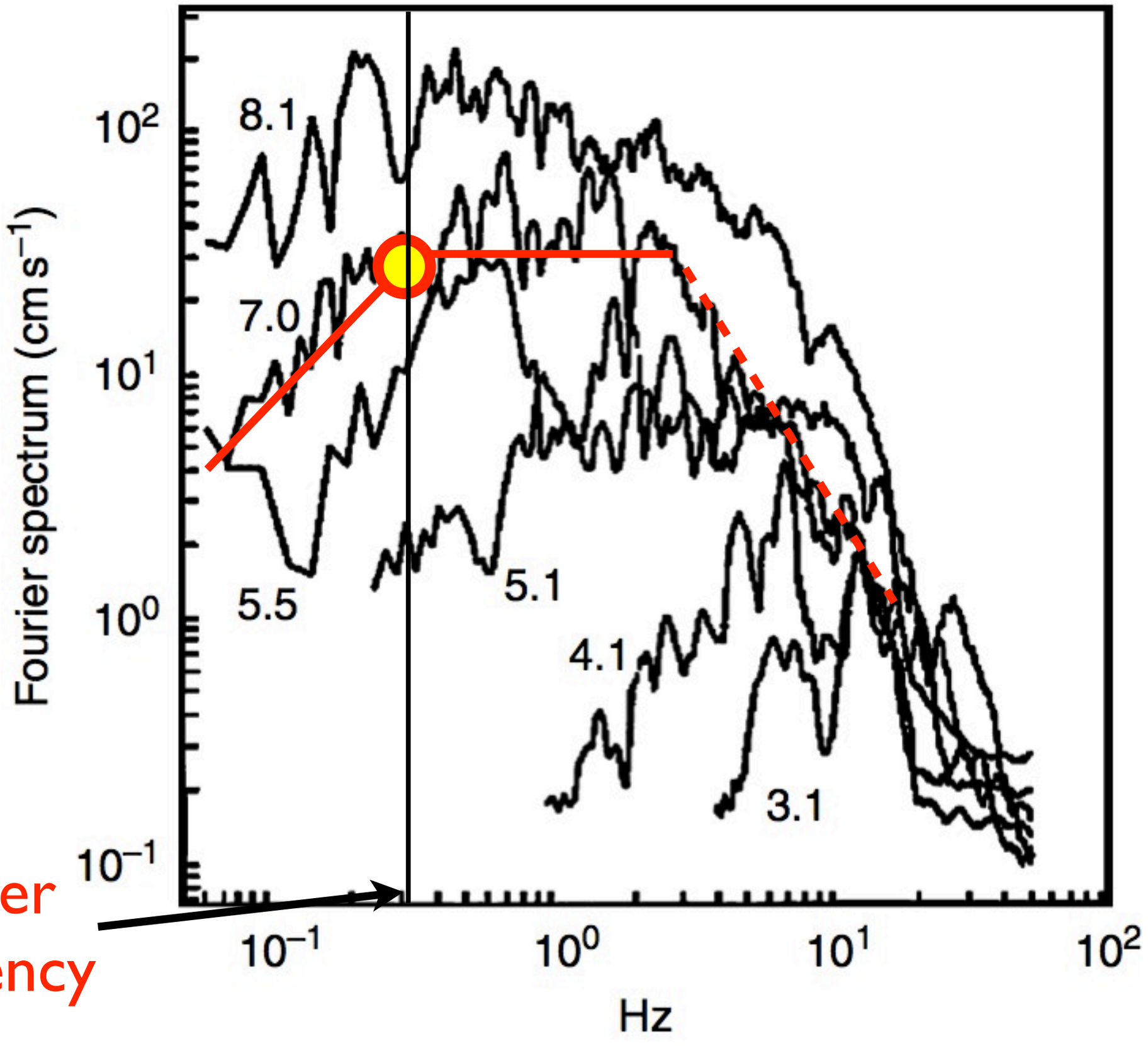

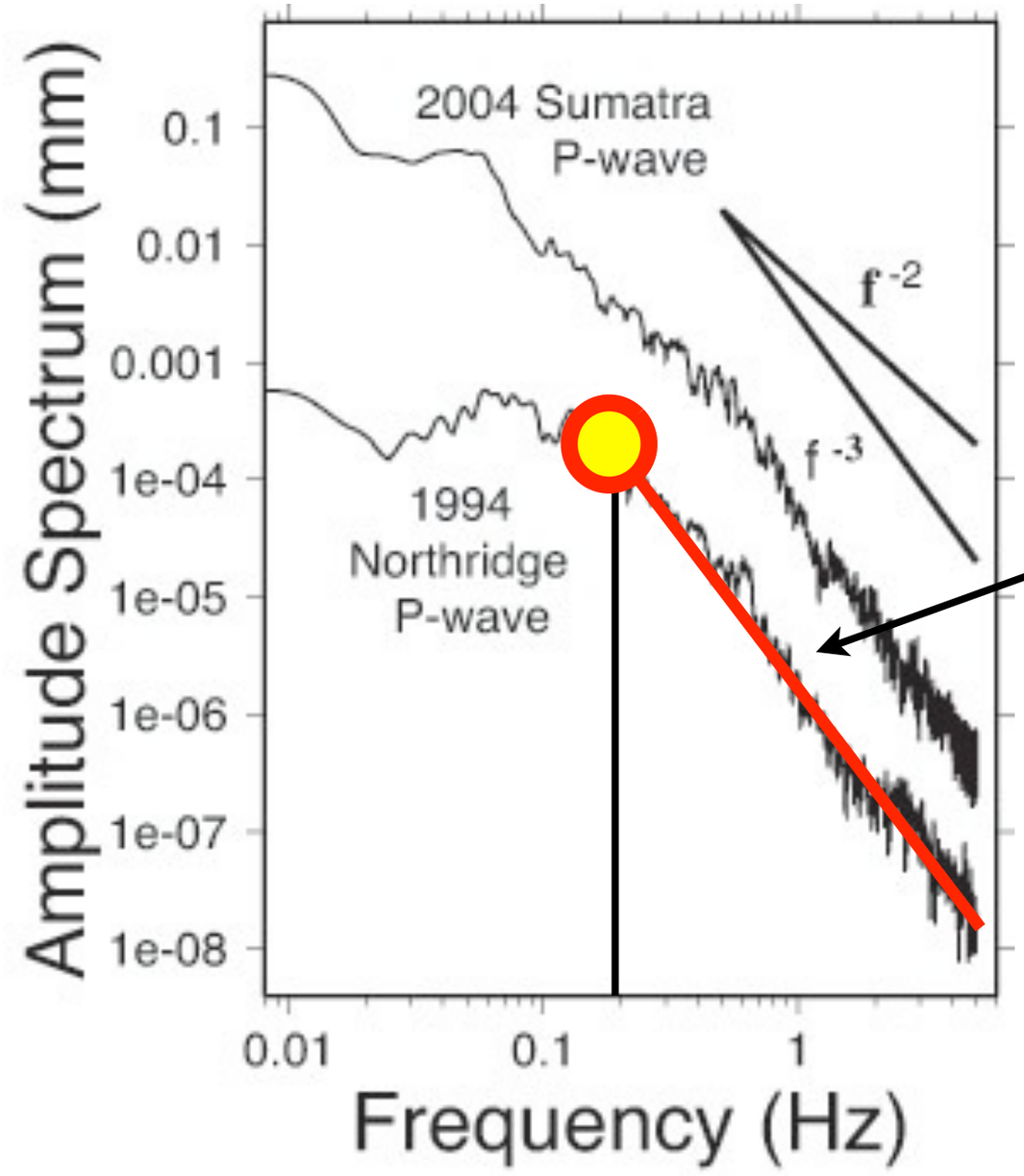

$$|\tilde{a}_{(f)}| = (2\pi f)^2 |\tilde{u}_{(f)}|$$

so the flat part of the acceleration spectrum has a slope of -2 on this displacement spectrum plot

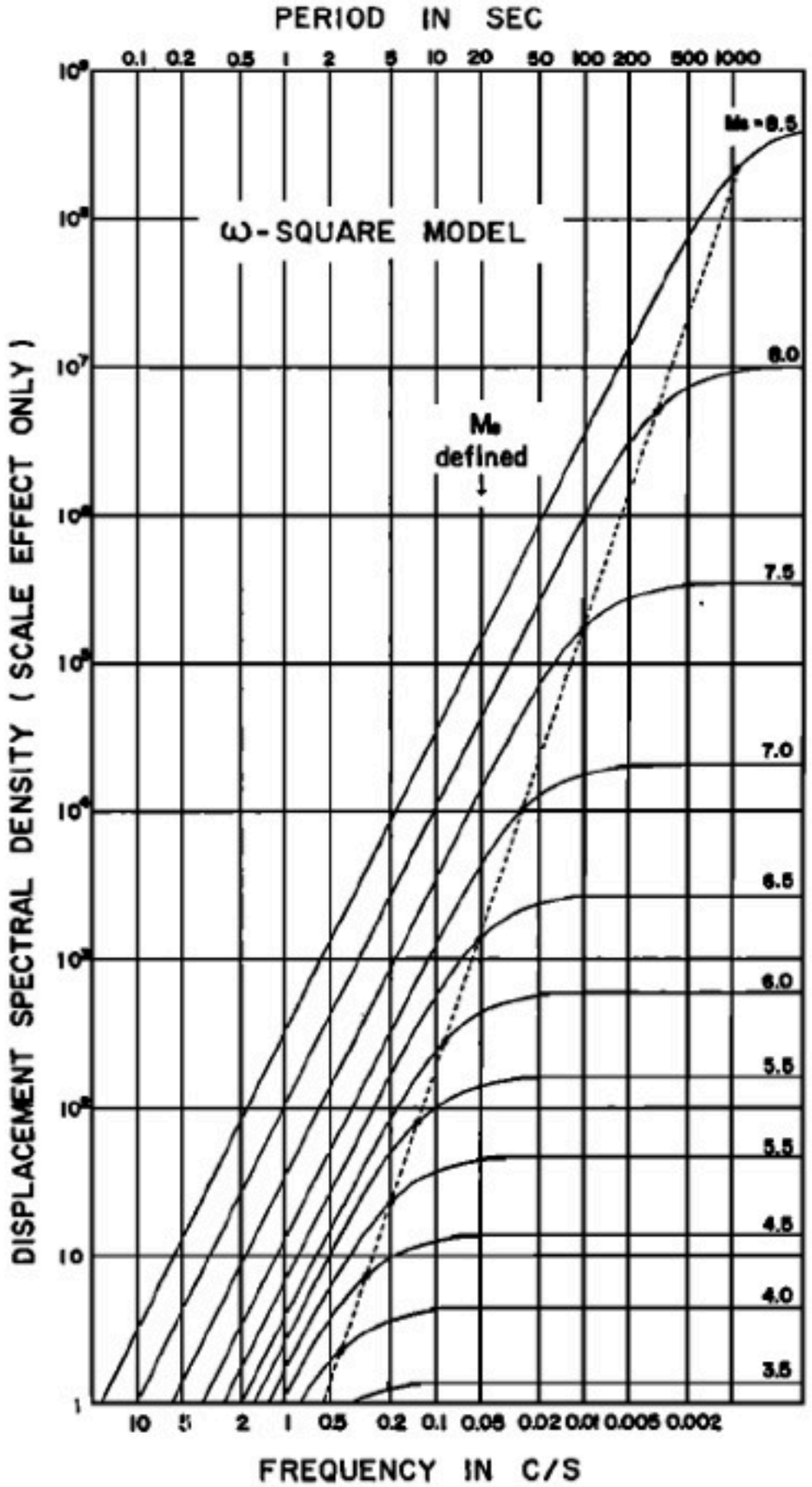

Fig. 3. Dependence of amplitude spectral density of earthquake magnitude M, for the ω-square model.

Aki, 1967

Displacement spectrum

example: M 6

Fc = _____ Hz

$$r = \frac{2.34\beta}{2\pi f_c}$$

$$\Delta\sigma = \frac{7}{16}\frac{M_o}{r^3}$$

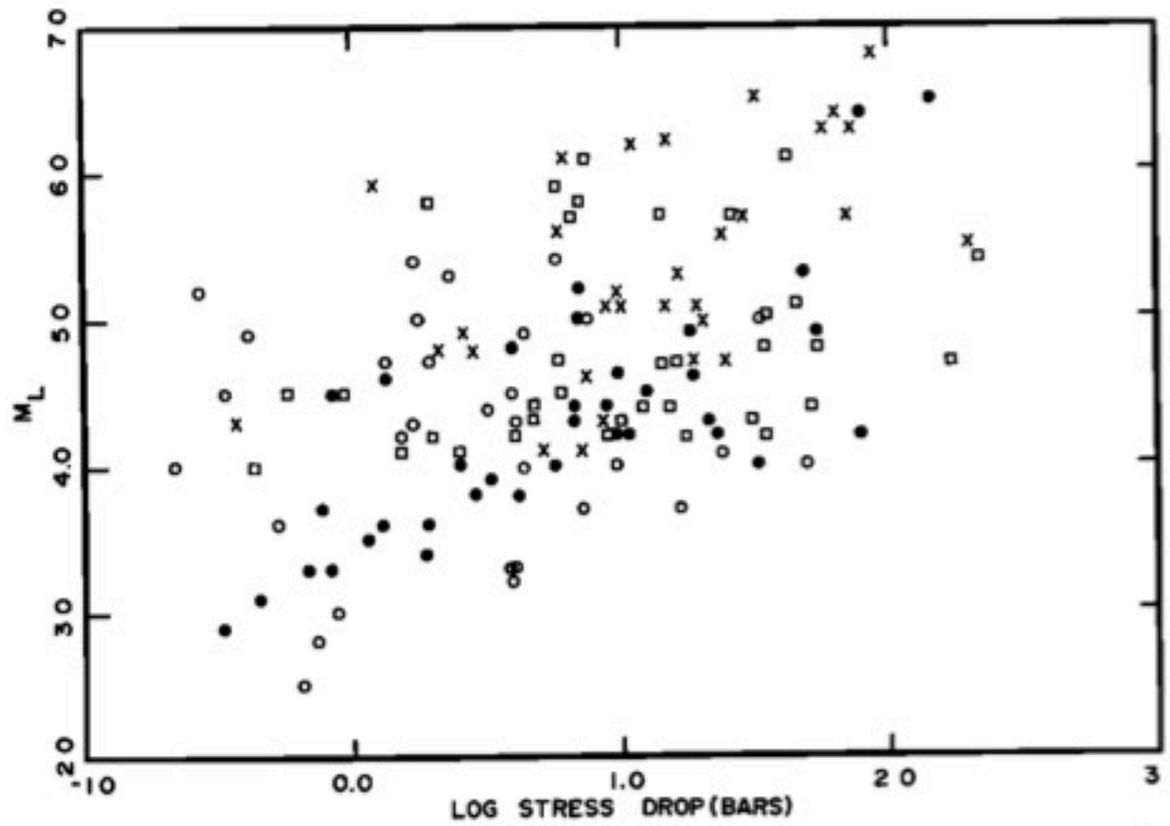

Fig. 9. Local magnitude versus log stress drop. Open circles represent earthquakes in offshore province and San Andreas fault; solid circles, in Transverse Ranges; squares, in Kern county; crosses, in other southern California locations.

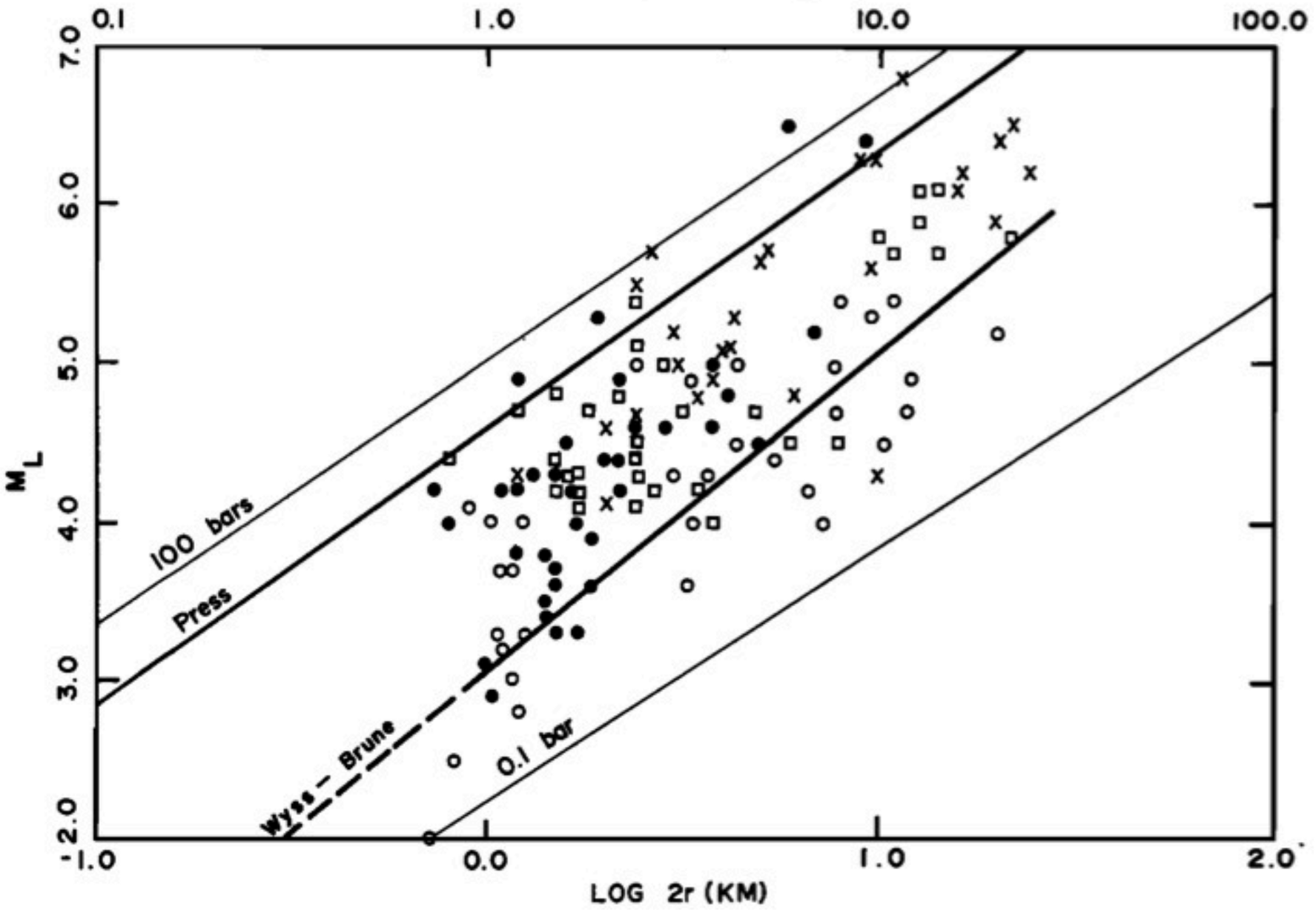
Source Dimension (km)
0.1
1.0
10.0
100.0
7.0
6.0
5.0
4.0
3.0
2.0
M_L
100 bars
Press
Wyss – Brune
0.1 bar
-1.0
0.0
1.0
2.0
LOG 2r (KM)

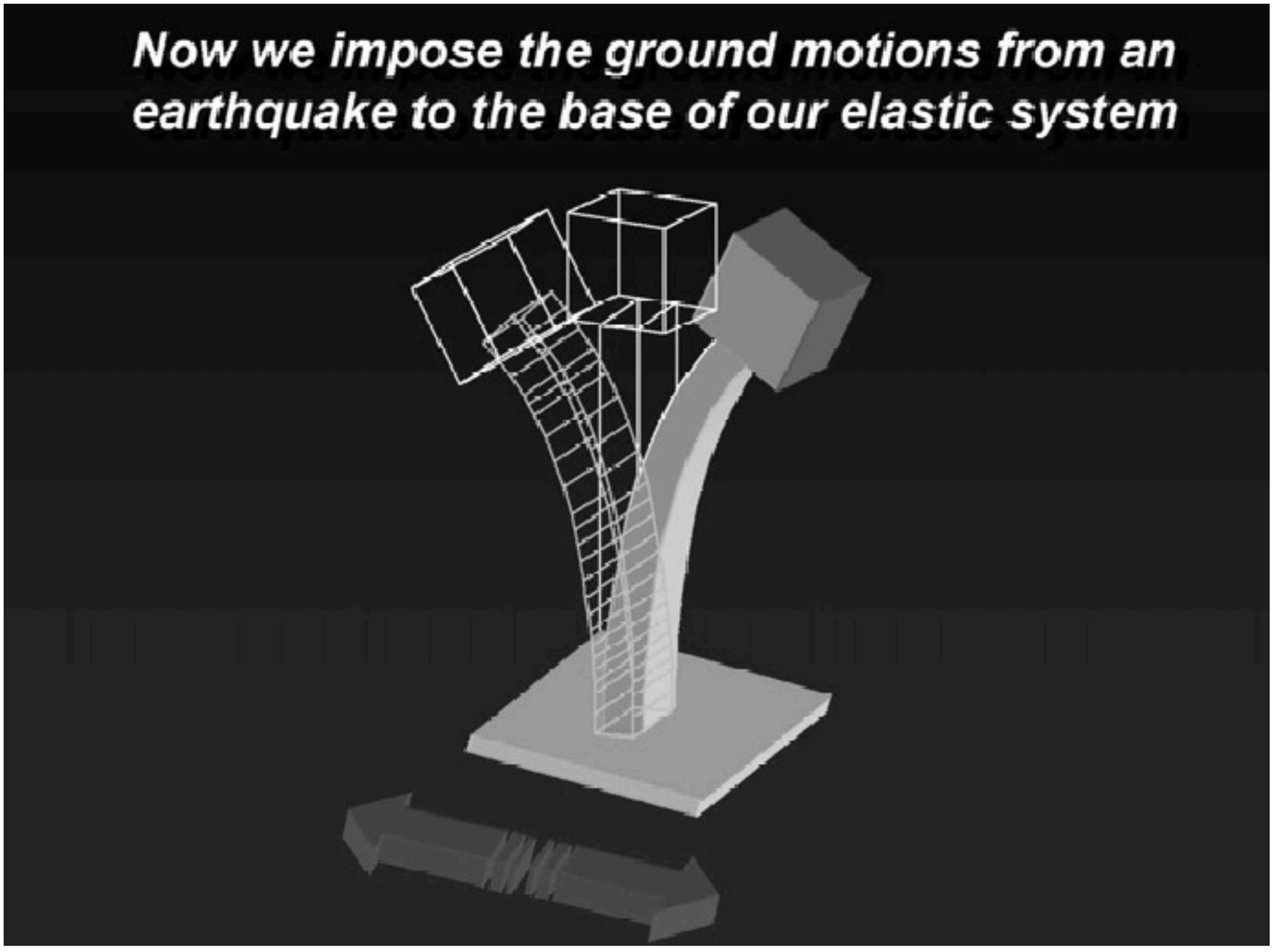
Now we impose the ground motions from an earthquake to the base of our elastic system

- Single-degree-of-freedom oscillators

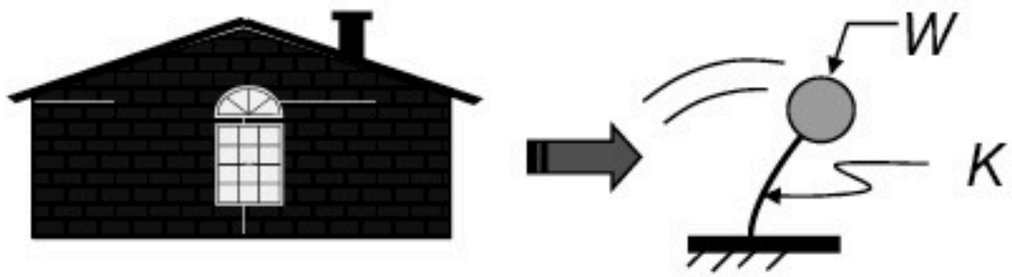

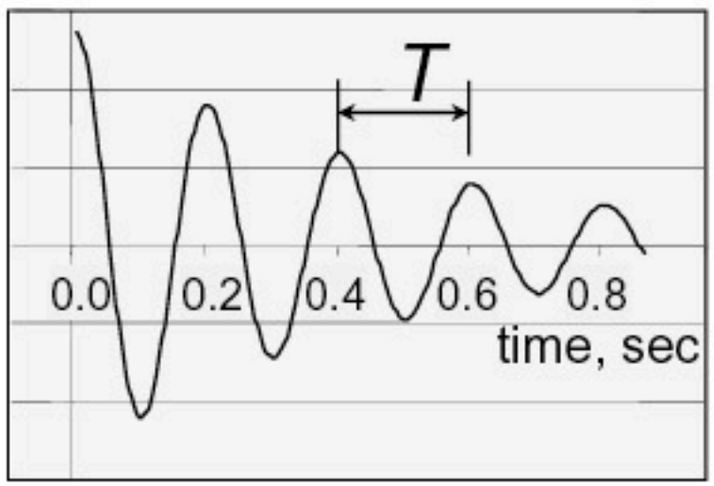

Vibration Period

$$T = \sqrt{\frac{m}{k}}$$

Base excitation

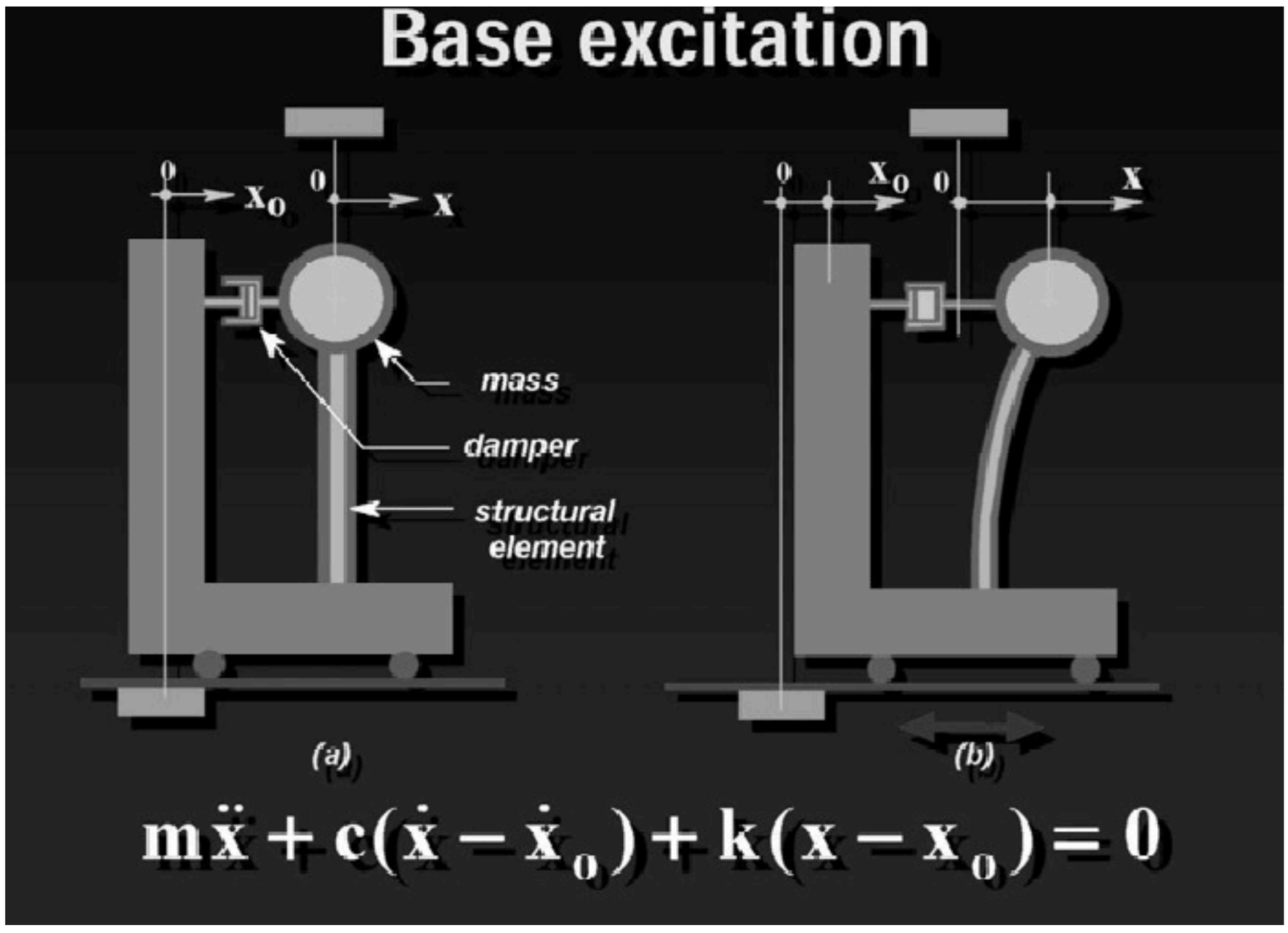

$$m\ddot{x} + c(\dot{x} - \dot{x}_0) + k(x - x_0) = 0$$

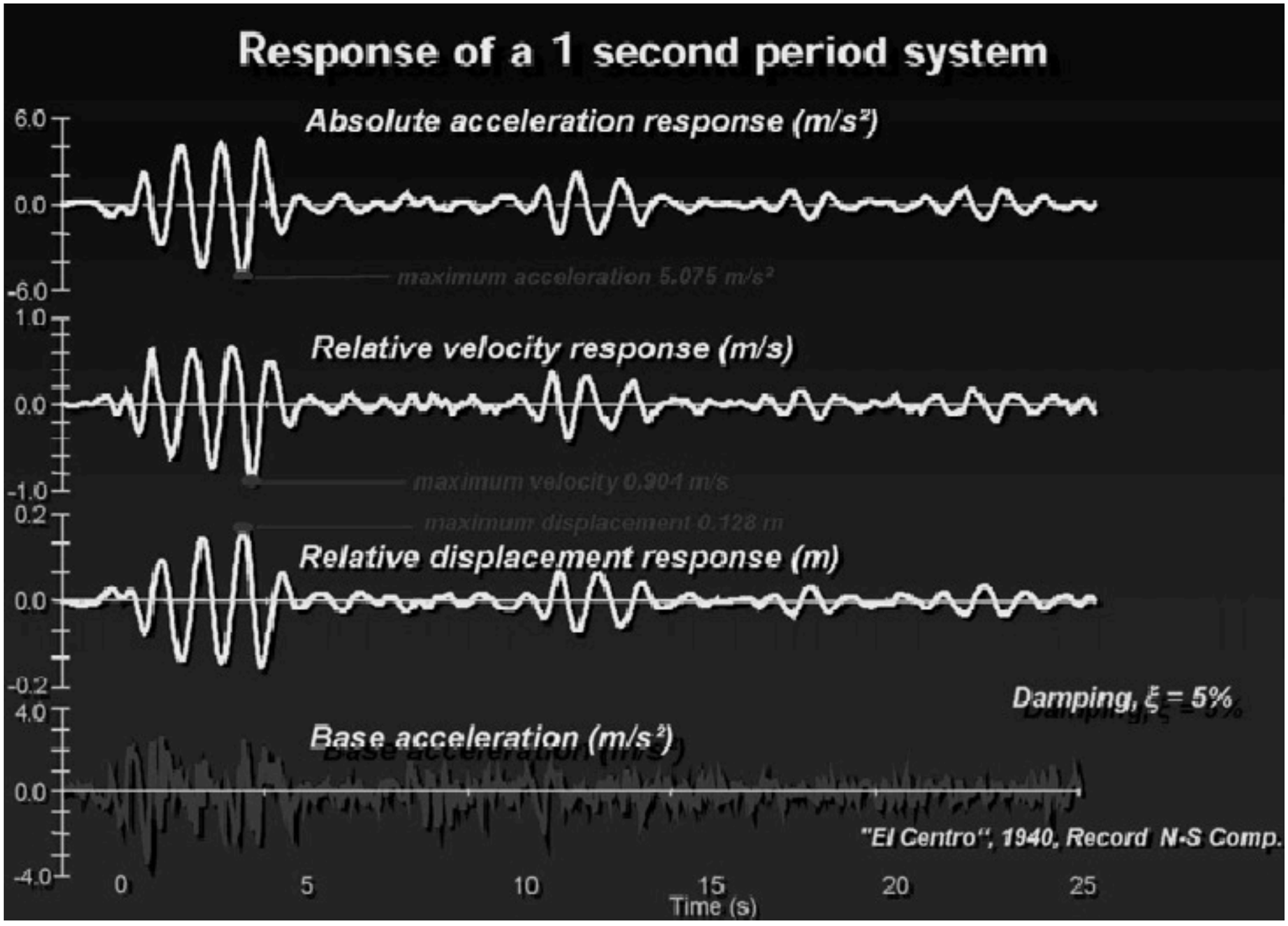
Response of a 1 second period system
Absolute acceleration response (m/s²)
6.0
0.0
-6.0
maximum acceleration 5.075 m/s²
Relative velocity response (m/s)
1.0
0.0
-1.0
maximum velocity 0.904 m/s
Relative displacement response (m)
0.2
0.0
-0.2
maximum displacement 0.128 m
Damping, ξ = 5%
Base acceleration (m/s²)
4.0
0.0
-4.0
"El Centro", 1940, Record N-S Comp.
0
5
10
15
20
25
Time (s)

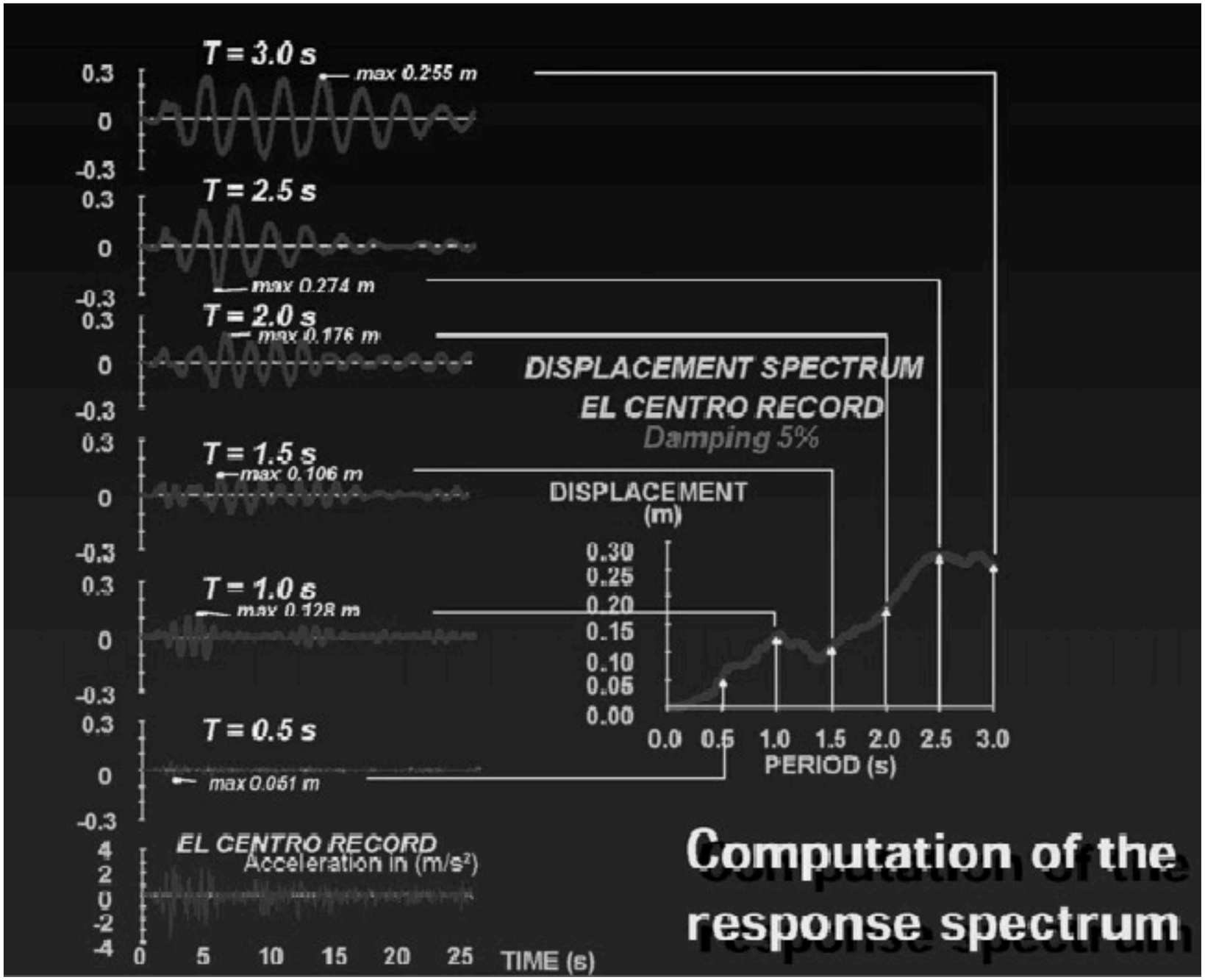
T = 3.0 s
max 0.255 m
T = 2.5 s
max 0.274 m
T = 2.0 s
max 0.176 m
T = 1.5 s
max 0.106 m
T = 1.0 s
max 0.128 m
T = 0.5 s
max 0.051 m
0.3
0
-0.3
EL CENTRO RECORD
Acceleration in (m/s²)
4
2
0
-2
-4
0
5
10
15
20
25
TIME (s)
DISPLACEMENT SPECTRUM
EL CENTRO RECORD
Damping 5%
DISPLACEMENT
(m)
0.30
0.25
0.20
0.15
0.10
0.05
0.00
0.0
0.5
1.0
1.5
2.0
2.5
3.0
PERIOD (s)
Computation of the
response spectrum

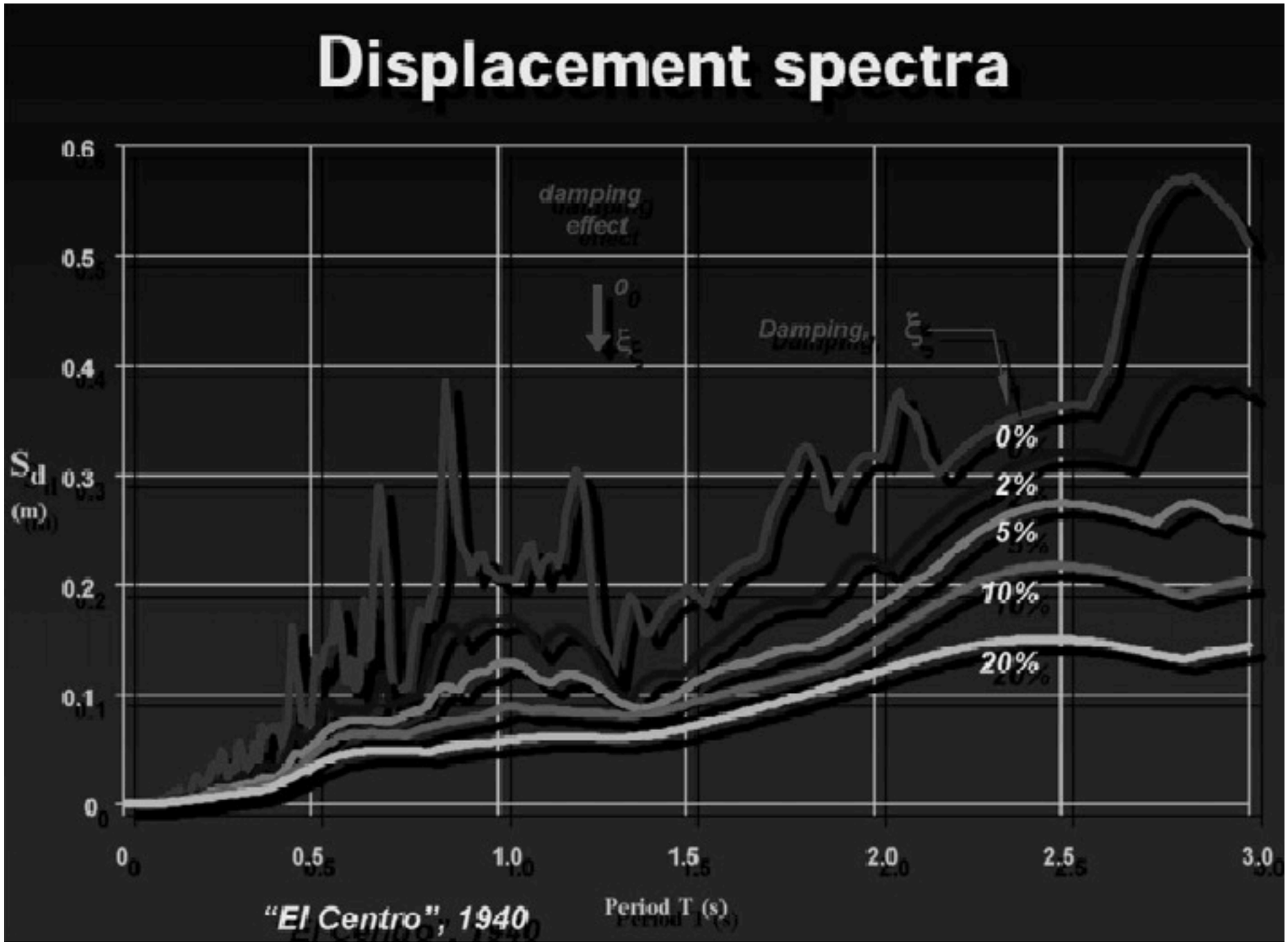
Displacement spectra
damping effect
Damping
0%
2%
5%
10%
20%
S_d (m)
0.6
0.5
0.4
0.3
0.2
0.1
0
0
0.5
1.0
1.5
2.0
2.5
3.0
Period T (s)
"El Centro", 1940

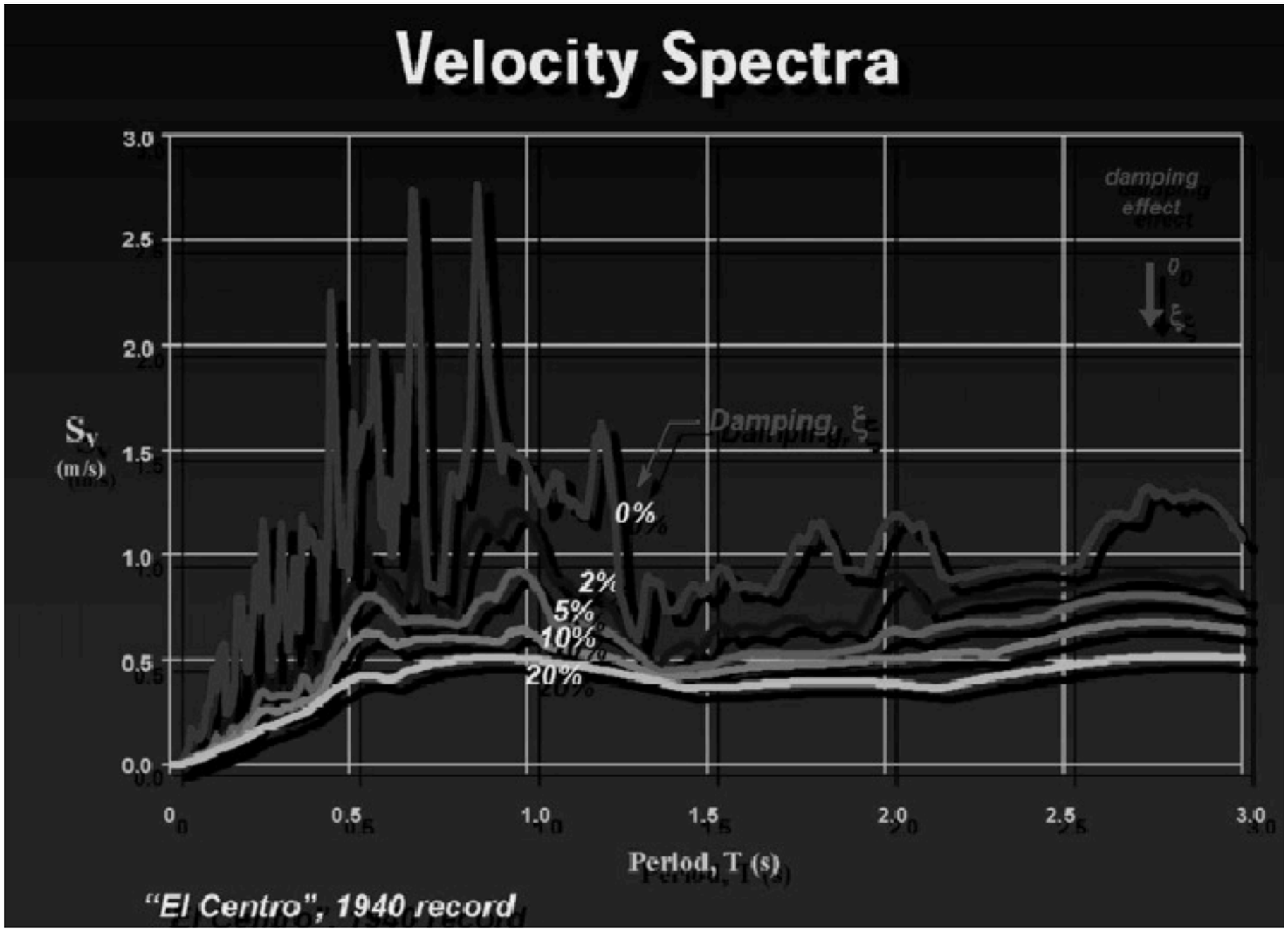
Velocity Spectra
3.0
2.5
2.0
1.5
1.0
0.5
0.0
Sv
(m/s)
damping
effect
Damping, ξ
0%
2%
5%
10%
20%
0
0.5
1.0
1.5
2.0
2.5
3.0
Period, T (s)
"El Centro", 1940 record

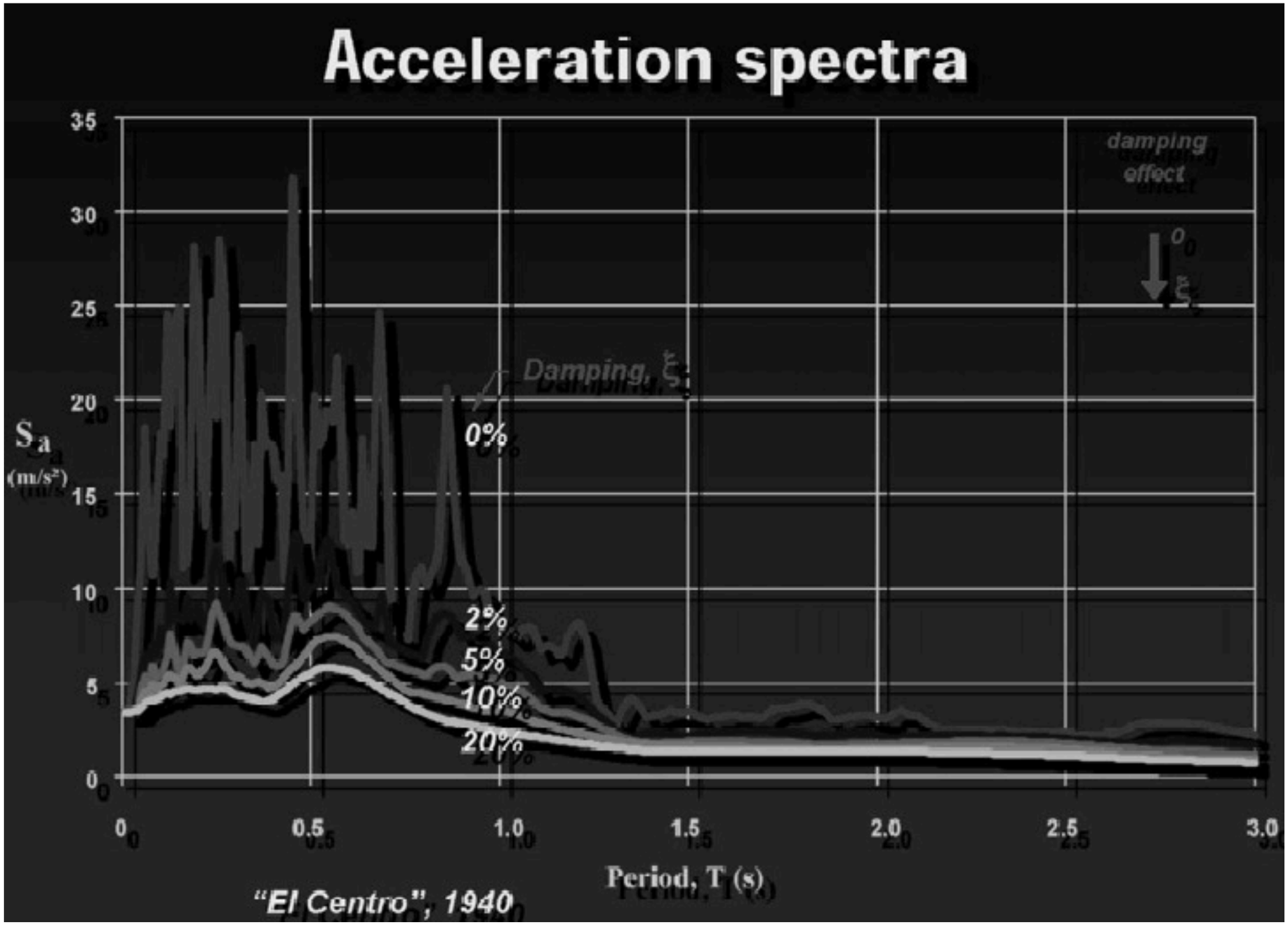
Acceleration spectra
damping effect
ξ_0
Damping, ξ
0%
2%
5%
10%
20%
S_a (m/s²)
35
30
25
20
15
10
5
0
0
0.5
1.0
1.5
2.0
2.5
3.0
Period, T (s)
"El Centro", 1940

Log-log plot of velocity spectra

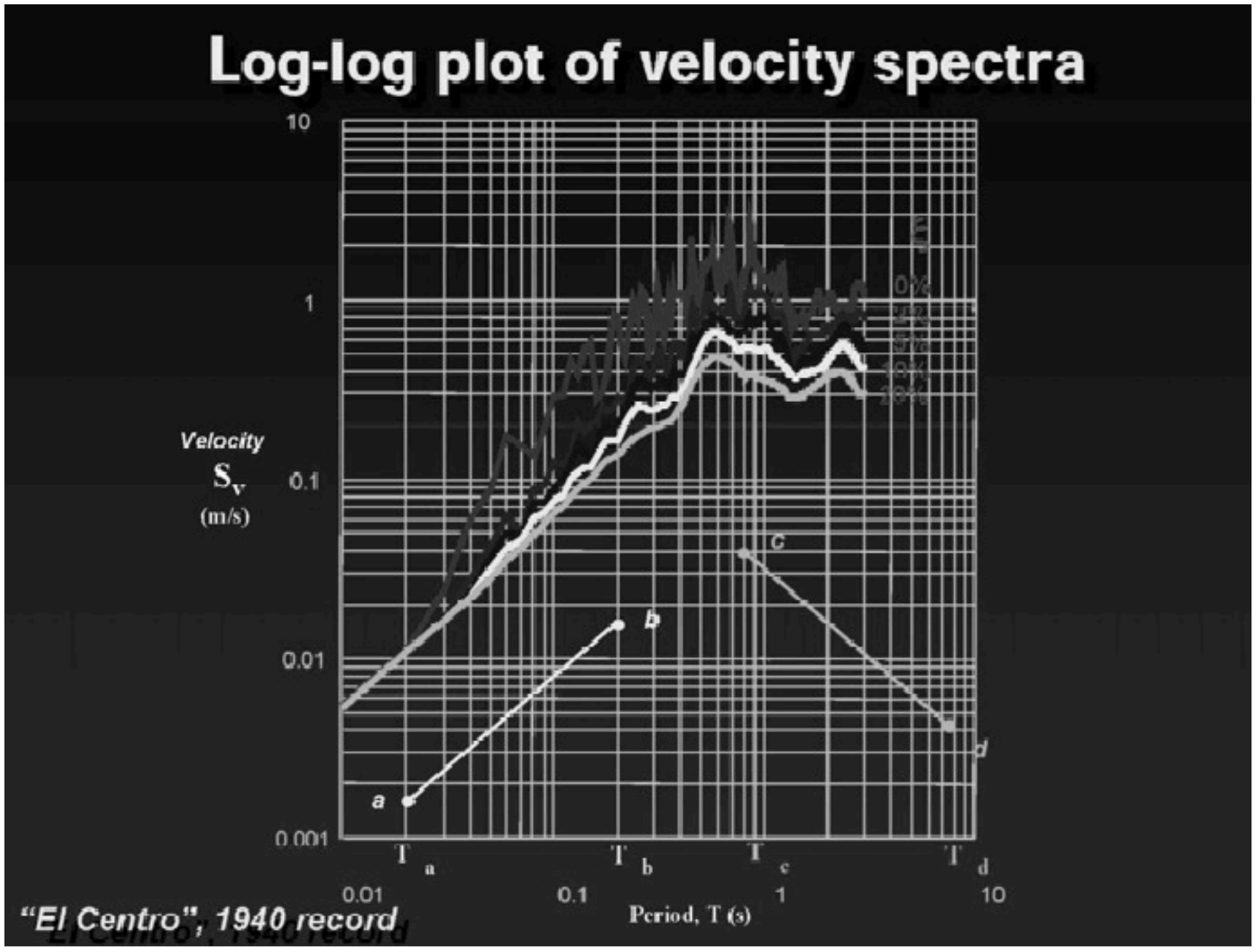

"El Centro", 1940 record

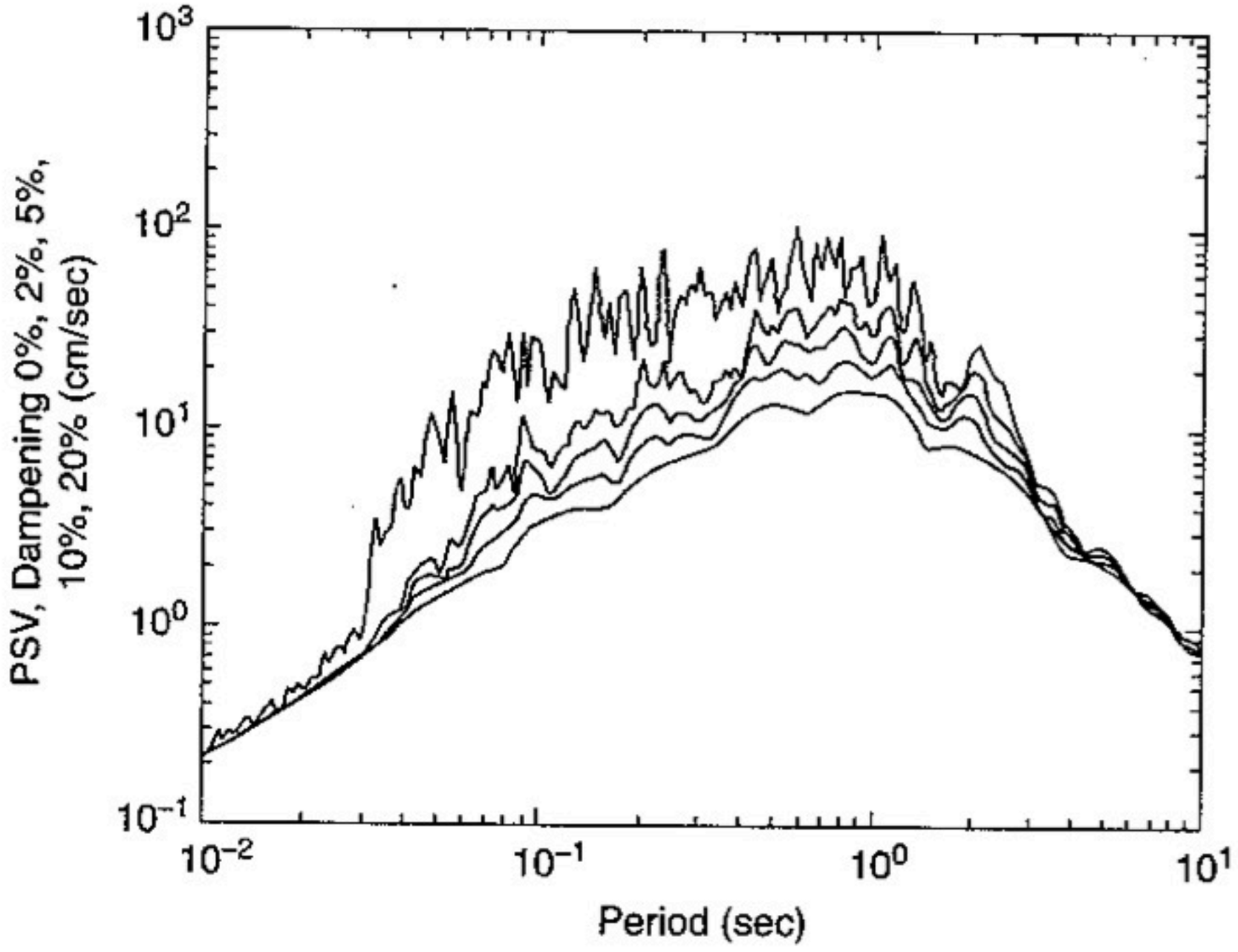

FIGURE 6 Pseudo-relative velocity response spectrum determined from the north–south component of acceleration recorded at Caleta de Campos during the September 19, 1985, Michoacan earthquake.

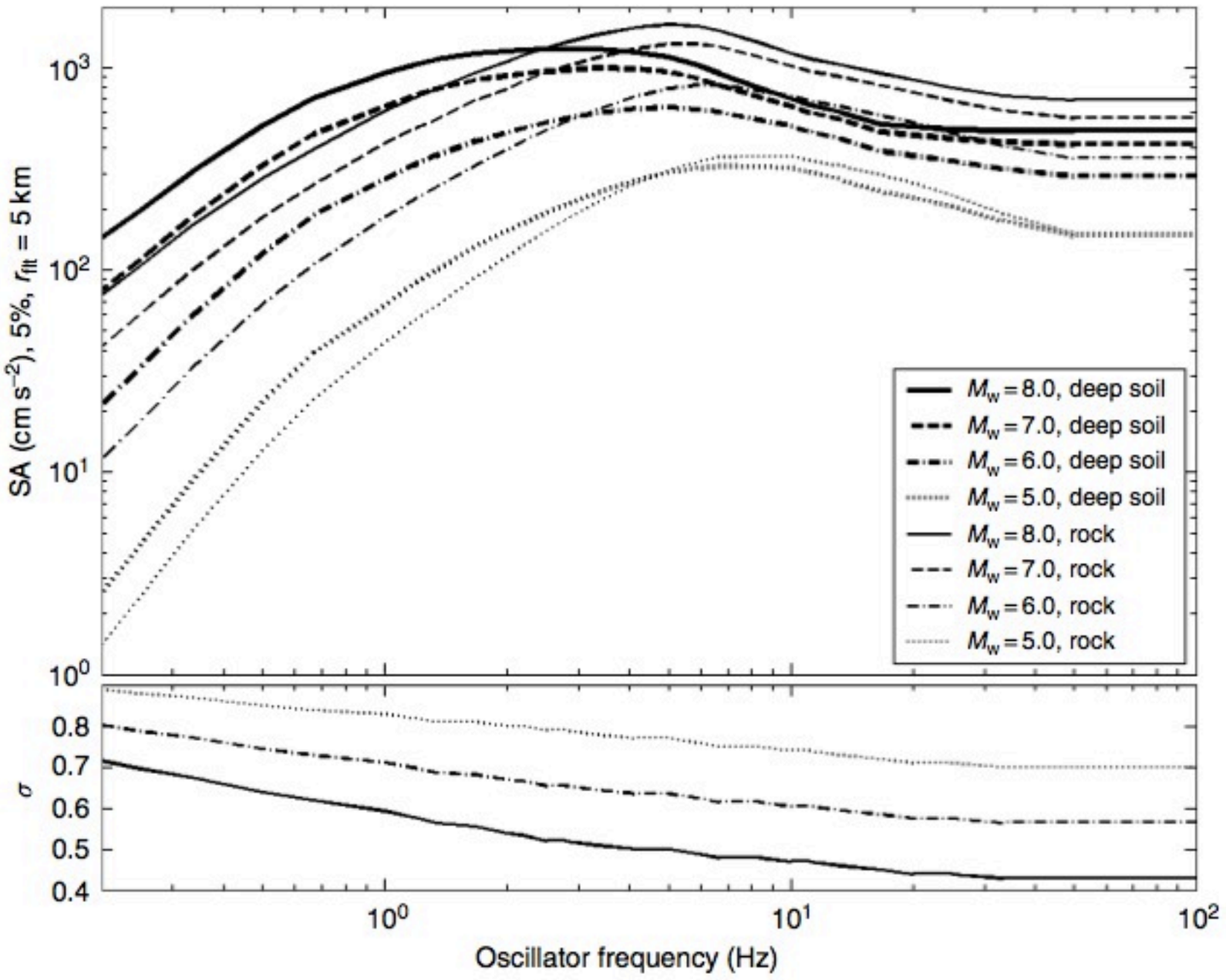

Figure 30 Ground motion predictions of Abrahamson and Silva (1997) for acceleration response spectra (SA) with 5% damping. The acceleration response at the oscillator frequency f_0 gives the peak response of a damped single-degree-of-freedom oscillator to the accelerogram. Because of its usefulness for approximating the response of a simple structure, SA is commonly used in engineering seismology instead of the Fourier spectrum (FS). At high frequencies, SA is assymptotic to peak acceleration, in contrast to the Fourier amplitude spectrum that falls off rapidly. At low frequencies, the assymptote is controlled by the peak displacement on the integrated accelerogram. At frequencies between those controlled by the assymptotes, SA is related to $(2\pi f_0)\mathrm{FS}(f_0)$ (Udwadia and Trifunac, 1973). At the bottom, the figure shows the standard deviation of the prediction equations, in natural logarithm units. In this model, the standard deviation is the same for both soil and rock sites, and the standard deviation for $M_W = 7$ is the same as for $M_W = 8$.

$$
\begin{aligned}
\mathbf{u}(\mathbf{x}, t) = & \frac{1}{4\pi\rho}\mathbf{A}^N \frac{1}{r^4}\int_{r/\alpha}^{r/\beta} \tau M_0(t-\tau)\,d\tau \\
& + \frac{1}{4\pi\rho\alpha^2}\mathbf{A}^{IP}\frac{1}{r^2}M_0\left(t-\frac{r}{\alpha}\right) \\
& + \frac{1}{4\pi\rho\beta^2}\mathbf{A}^{IS}\frac{1}{r^2}M_0\left(t-\frac{r}{\beta}\right) \\
& + \frac{1}{4\pi\rho\alpha^3}\mathbf{A}^{FP}\frac{1}{r}\dot{M}_0\left(t-\frac{r}{\alpha}\right) \\
& + \frac{1}{4\pi\rho\beta^3}\mathbf{A}^{FS}\frac{1}{r}\dot{M}_0\left(t-\frac{r}{\beta}\right), \qquad (8)
\end{aligned}
$$

where the radiation pattern terms are

$$
\begin{aligned}
\mathbf{A}^N &= 9\sin 2\theta\,\cos\varphi\hat{\mathbf{r}} \quad - 6(\cos 2\theta\,\cos\varphi\hat{\boldsymbol{\theta}} - \cos\theta\,\sin\varphi\hat{\boldsymbol{\varphi}}) \\
\mathbf{A}^{IP} &= 4\sin 2\theta\,\cos\varphi\hat{\mathbf{r}} \quad - 2(\cos 2\theta\,\cos\varphi\hat{\boldsymbol{\theta}} - \cos\theta\,\sin\varphi\hat{\boldsymbol{\varphi}}) \\
\mathbf{A}^{IS} &= -3\sin 2\theta\,\cos\varphi\hat{\mathbf{r}} + 3(\cos 2\theta\,\cos\varphi\hat{\boldsymbol{\theta}} - \cos\theta\,\sin\varphi\hat{\boldsymbol{\varphi}}) \\
\mathbf{A}^{FP} &= \sin 2\theta\,\cos\varphi\hat{\mathbf{r}} \\
\mathbf{A}^{FS} &= \qquad\qquad (\cos 2\theta\,\cos\varphi\hat{\boldsymbol{\theta}} - \cos\theta\,\sin\varphi\hat{\boldsymbol{\varphi}}).
\end{aligned} \qquad (9)
$$